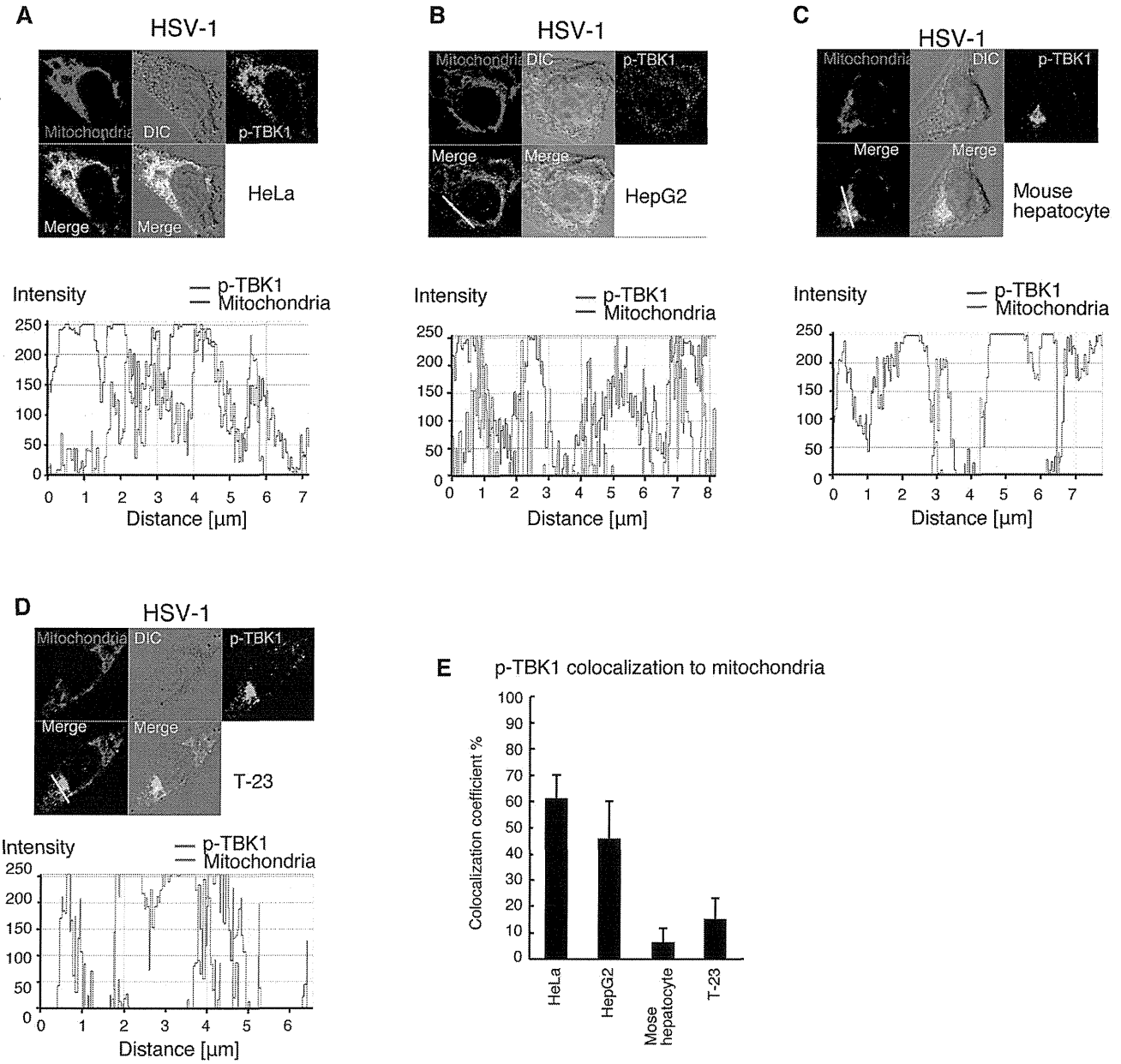

Figure 8. p-TBK1 localization in response to HSV-1 infection. HeLa (A), HepG2 (B), mouse hepatocyte (C), and T-23 (D) cells were infected with HSV-1 for 24 h. Cells were fixed and stained with Mitotracker Red and anti-p-TBK1 antibody. Histograms display the measured fluorescence intensity along the white line in the merged panels. Colocalization coefficients of p-TBK1 to mitochondria are shown (E).

doi: 10.1371/journal.pone.0083639.g008

Next, we investigated whether siRNA for *IPS-1* or *STING* reduces IFN-β mRNA expression in response to DNA stimulation. siRNA for *IPS-1* significantly reduced IFN-β mRNA expression in response to vertebrate DNA and HBV DNA F1 fragment in HeLa cells (Figure 9D), whereas siRNA for *IPS-1* failed to reduce IFN-β mRNA expression in response to vertebrate DNA in L929 cells (Figure S3B). siRNA for *STING* also reduced IFN-β mRNA expression in HeLa cells (Figure 9D). Taken together, these data indicated that IPS-1, as well as STING, are required for TBK1 phosphorylation and efficient IFN-β mRNA expression in response to cytoplasmic DNA in HeLa cells.

Next, we compared dsDNA-induced type I IFN mRNA expressions among human and mouse cells. HeLa cells were less responsive to DNA stimulation compared to THP-1, L929, and RAW264.7 cells (Figure 10A). Therefore, there is a

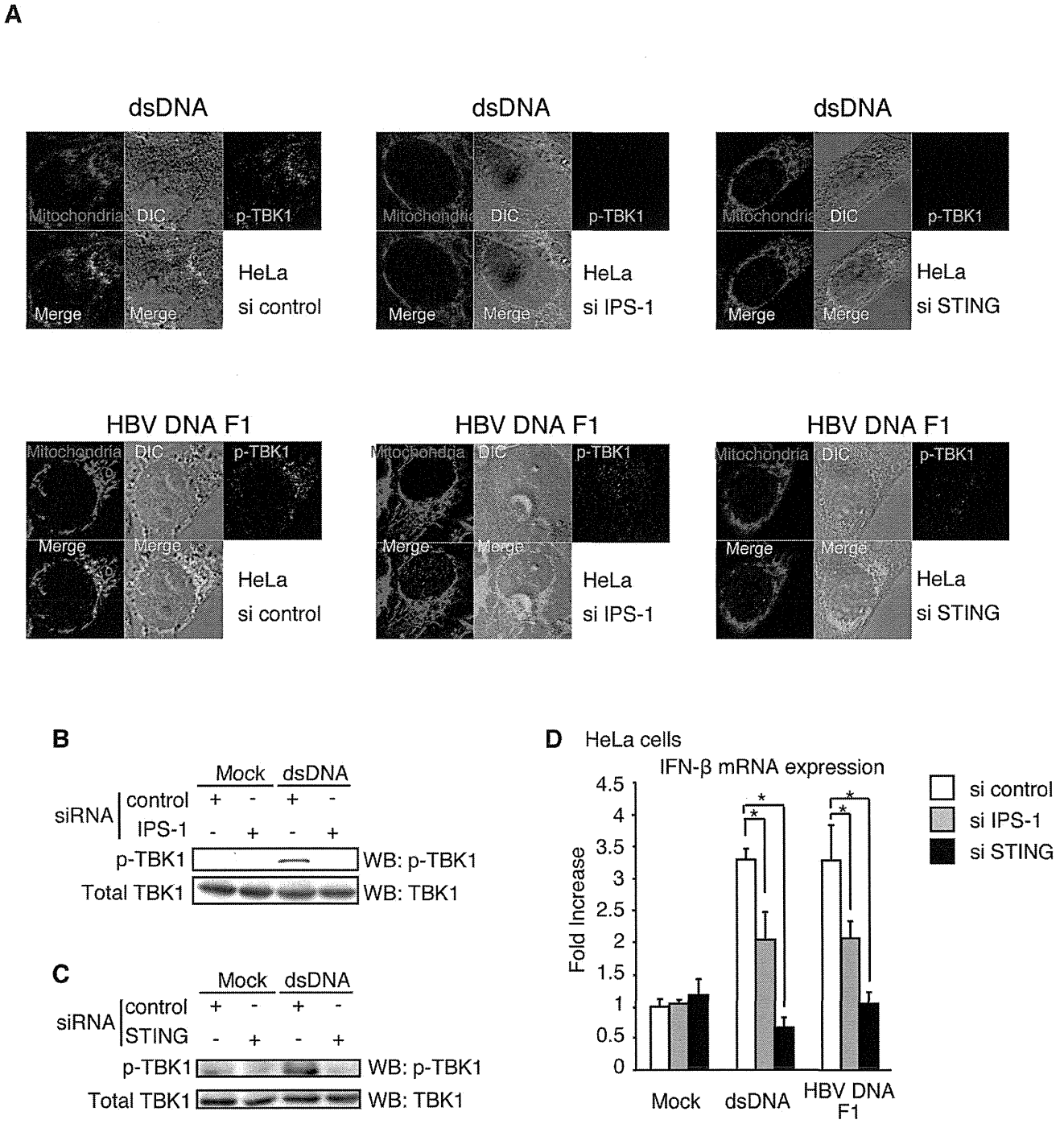

Figure 9. p-TBK1 levels in IPS-1 or STING knockdown cells. (A-C) siRNA for negative control, IPS-1, or STING were transfected into HeLa cells. At 48 h after transfection, cells were stimulated with HBV F1 fragment or salmon sperm DNA for 6 h. Cells were fixed and stained with Mitotracker Red and anti-p-TBK1 antibody (A), or cell lysates were prepared and subjected to SDS-PAGE and western blotting (B and C).

(D) siRNA for IPS-1 or STING were transfected into HeLa cells At 48 h after transfection, cells were stimulated with mock, HBV F1 fragment, or salmon sperm DNA (dsDNA) for 6 h. The IFN-β mRNA expression was determined by RT-qPCR.

doi: 10.1371/journal.pone.0083639.g009

possibility that mitochondrial localization might correlate with a lack of strong response of the cells to the cytoplasmic DNA stimulation. To test this possibility, we investigated p-TBK1 subcellular localization in THP-1, which efficiently expressed IFN-β mRNA in response to DNA stimulation as L929 cells (Figure 10A). p-TBK1 showed mitochondrial localization in response to salmon sperm DNA or HBV F1 DNA fragment in THP-1 cells (Figure 10B). This observation weakened the possibility.

Discussion

Autophosphorylation of TBK1 is essential for Type I IFN expression [28]. Here, we demonstrated that p-TBK1 is localized on mitochondria in response to cytoplasmic DNA in HeLa and HepG2 cells. p-TBK1 induced by DNA stimulation in HeLa and HepG2 cells co-localized with IPS-1 and MFN-1. Moreover, knockdown of *IPS-1* reduced p-TBK1 levels in response to viral DNA in HeLa cells. These data indicate that IPS-1 plays a crucial role in the phosphorylation of TBK1 in response to cytoplasmic DNA in the human cells. In contrast, p-TBK1 did not localize on mitochondria in the mouse or tree shrew cells that we tested. This is consistent with a previous knockout mouse study that showed that IPS-1 is dispensable for the response to cytoplasmic DNA [33]. Thus, there appears to be species-specific mechanisms of Type I IFN production in response to cytoplasmic DNA. However, we do not exclude the possibility that some of human primary or immortalized cells do not exhibit IPS-1 mitochondrial localization in response to cytoplasmic viral DNA. Taniguchi and colleagues firstly reported cell type-specific roles of a DNA sensor, DAI, in a cytoplasmic DNA sensing pathway [32,37]. Later, other groups reported several other DNA sensors using various types of cells [38]. Recently Chen and colleagues showed that cGAS is essential for type I IFN production in response to poly(dA:dT) in plasmacytoid DC but not in lung fibroblasts [39]. Their findings suggested that RNA polymerase III – RIG-I pathway plays a major role in sensing DNA in lung fibroblasts [24]. Thus, these observations indicate that there are several cell type-specific DNA sensing pathways. Our observations of cell type-specific p-TBK1 localization in response to cytoplasmic DNA also support this model.

Gale and colleagues previously reported that a major site of IPS-1 signaling is MAMs [8]. TBK1 autophosphorylation in response to HBV DNA required both IPS-1 and STING in human cells that we tested. Considering that IPS-1 and STING localize on the mitochondria and ER, respectively, it is expected that TBK1 autophosphorylation occurs within MAMs where the ER associates with mitochondria in response to cytoplasmic viral DNA in HeLa and HepG2 cells. Indeed, a fraction of cellular p-TBK1 was localized on MAMs. It is likely that TBK1 moved to mitochondria after autophosphorylation in human cells. In contrast, mouse and tree shrew TBK1 appears to be phosphorylated on ER where STING localizes. The biological significance of the mitochondrial or ER localization of p-TBK1 is unclear. A previous report demonstrated that peroxisomal IPS-1 triggers rapid expression of ISGs, whereas mitochondrial IPS-1 triggers delayed ISG and IFN expression

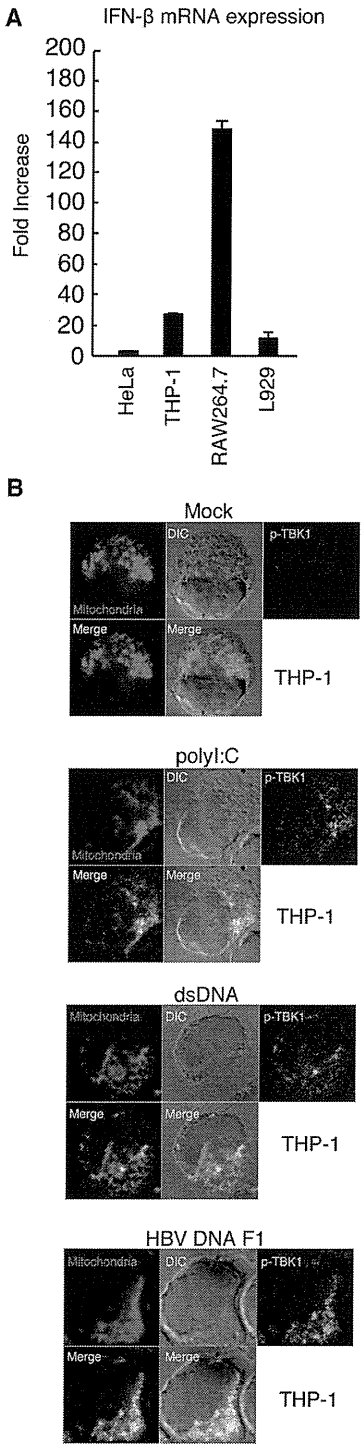

Figure 10. Subcellular localization of p-TBK1 in response to polyI:C or DNA in THP-1 cells. (A) HeLa, THP-1, Raw264.7, and L929 cells were stimulate with salmon sperm DNA for 6 h by transfection. The fold increase of IFN-β mRNA expression in response to DNA was determined by RT-qPCR. (B) THP-1 cells were stimulated with mock, polyI:C, salmon sperm DNA (dsDNA), or HBV DNA F1 for 3 h. Cells were fixed and stained with Mitotracker Red and anti-p-TBK1 antibody.

doi: 10.1371/journal.pone.0083639.g010

[7]. Thus, as observed with IPS-1, differential p-TBK1 placement may allow the cell to diversify signaling pathways.

When human STING or IPS-1 were transfected into mouse cells, p-TBK1 did not localize on the mitochondria in response to cytoplasmic DNA. Thus, the differences in the STING and IPS-1 protein sequences between humans and mice are not a cause of the cell type-specific localization of p-TBK1. It is possible that the difference in TBK1 protein sequence between humans and mice determines the cell type specific localization of p-TBK1. Another possibility is that an unknown factor of human or mouse associate with TBK1 or p-TBK1. Our current knowledge cannot explain the cell type-specific localization of p-TBK1 in response to cytoplasmic DNA stimulation. Further study is required to reveal the precise mechanisms used by cytoplasmic DNA sensing pathways.

Materials and Methods

Cells, viruses, and reagents

A tree shrew (*Tupaia belangeri*) fibroblast cell line, T-23 (clone 8) cells were obtained from JCRB. T-23 and HepG2 cells were cultured in Dulbecco's modified Eagle's medium low glucose medium (D-MEM) with 10% heat-inactivated fetal calf serum (FCS) (Invitrogen). HeLa cells were cultured in minimum Eagle's medium with 2 mM L-glutamine and 10% heat-inactivated FCS. Protocols for the isolation and culture conditions of mouse hepatocytes have been described previously [34]. L929 and RAW264.7 cells were cultured in RPMI1640 with 10% of FCS. Salmon sperm DNA and polyI:C were purchased from Invitrogen or GE Healthcare, respectively. HSV-1 K strain was amplified using Vero cells. To determine viral titers, we performed plaque assay using Vero cells. Vero cells were cultured in D-MEM with 10% of FCS. THP-1 cells were cultured in RPMI1640 with 10 % FCS and 0.1 % 2-mercaptoethanol.

Confocal Microscopy

Phospho-TBK1/NAK (Ser 172) (D52C2) XP rabbit mAb were purchased from Cell Signaling. Anti-Presenilin 1 Ab [APS11], anti-NAK (TBK1) Ab (EP611Y), anti-mitofusin 1 Ab, and anti-G3BP Ab were purchased from Abcam. Anti-FLAG antibody was purchased from Sigma-Aldrich. Anti-HA Ab [HA1.1] was purchased from COVANCE. Mitotracker Red was purchased from Life Technologies. Cells were fixed with 3% of formaldehyde in 1x PBS for 30 min, and permeabilized with 0.2% Triton X-100 in 1 x PBS for 15 min. In case of PSEN-1 staining, fixed cells were permeabilized with 0.5% of saponin in 1x PBS with 1 % BSA for 30 min. For blocking, 1% BSA in PBS was used for 30 min. The cells were labeled with the indicated primary antibody for 60 min at room temperature. After washing four times with 1% BSA in PBS, cells were incubated with an Alexa-conjugated secondary antibody and 1% BSA in PBS for 30 min at room temperature, and then were washed four times with 1% BSA in PBS. Samples were mounted on glass slides using Prolong Gold (Invitrogen). Cells were visualized at a magnification of ×63 with an LSM510 META microscope (Zeiss). Colocalization of coefficients and intensity histograms were determined using LSM510 ZEISS LSM Image examiner software.

Plasmids

RIG-I CARDs expression vector (dRIG-I) has been described previously [40]. Human *IPS-1* cDNA encoding the full-length ORF was cloned into a pEF-BOS multi-cloning site, and an HA sequence was inserted just before the STOP codon. Human *STING* cDNA that encoded a full-length ORF was cloned into a pEF-BOS multi-cloning site, and a FLAG-tag sequence was inserted just before the STOP codon. The plasmids were sequenced to confirm that there were no PCR errors.

HBV DNA preparation and quantitative PCR

HBV DNA fragments were obtained by PCR using HBV DNA as a template. A plasmid carrying HBV full-length genomic DNA were kindly gifted from Chayama K. Primer sequences were as follows: F1 forward, TGC AAC TTT TTC ACC TCT GC; F1 reverse, TCT CCT TTT TTC ATT AAC TG; F2 forward, TTA AAA TTA ATT ATG CCT GC; F2 reverse, AAC AAG AAA AAC CCC GCC TG; F3 forward, GAC AAG AAT CCT CAC AAT AC; F3 reverse, TGT ACA ATA TGT TCT TGT GG; F4 forward, AAA AAT CAA GCA ATG TTT TC; and F4 reverse, ATT AGG CAG AGG TGA AAA AG. Amplified DNA fragments were purified using a Gel Extraction kit (Qiagen). For quantitative PCR (qPCR), total RNA was extracted using TRIZOL reagent (Invitrogen), after which 0.1-1 μg of RNA was reverse-transcribed using a high capacity cDNA transcription kit with an RNase inhibitor kit (Applied Biosystems) according to the manufacturer's instructions. qPCR was performed using a Step 1 real time PCR system (Applied Biosystems). The expression of cytokines mRNA was normalized to that of *GAPDH* or *β-actin* mRNA, and the fold-increase was determined by dividing the expressions in each sample by that of the wild-type at 0 h. The primers used for qPCR were described previously [40,41].

Supporting Information

Figure S1. HeLa cells were transfected with HA-tagged IPS-1 (A) or FLAG-tagged STING (B). At 24 h after transfection, cells were mock-stimulated for 6 h, and then fixed and stained with anti-p-TBK1 and HA or FLAG Abs.
(TIF)

Figure S2. HepG2 cells were transfected with a vector carrying 1.4 x HBV genomic DNA. Total RNA was extracted at indicated hours. IFN-β mRNA expression was determined by RT-qPCR.
(TIF)

Figure S3. siRNAs for control, IPS-1, or STING were transfected into HeLa and L929 cells. 48 h after transfection, cells were stimulated with or without dsDNA for 6 h. Total RNA was extracted with TRIZOL, and RT-qPCR was performed. IPS-1 and STING mRNA expressions were normalized with β-actin mRNA expression. Relative ratio was calculated by

dividing each ratio by the ratio of the "mock si control" sample. The target sequences of siRNA for human *IPS-1* and *STING* are: CCA AAG UGC CUA CCA CCU U and GGA UUC GAA CUU ACA AUC A, respectively. The target sequence of siRNA for mouse *IPS-1* and *STING* are: UGU□UGC□CUC□UGU□ UCC□CAUA and GCA CAU UCG UCA GGA AGA A, respectively. Silencer Select siRNAs were purchased from Life Technologies.
(TIF)

Acknowledgements

Plasmids carrying HBV genomic DNA were kindly gifted from Chayama K (Hiroshima University, Japan) and Chisari FV (The Scripps Research Institute, USA).

Author Contributions

Conceived and designed the experiments: HO M. Matsumoto T. Seya. Performed the experiments: T. Suzuki HO M. Miyashita. Analyzed the data: T. Suzuki HO M. Miyashita. Contributed reagents/materials/analysis tools: HA. Wrote the manuscript: HO T. Seya.

References

1. Loo YM, Gale M Jr. (2011) Immune signaling by RIG-I-like receptors. Immunity 34: 680-692. doi:10.1016/j.immuni.2011.05.003. PubMed: 21616437.
2. Onomoto K, Jogi M, Yoo JS, Narita R, Morimoto S et al. (2012) Critical role of an antiviral stress granule containing RIG-I and PKR in viral detection and innate immunity. PLOS ONE 7: e43031. doi:10.1371/journal.pone.0043031. PubMed: 22912779.
3. Xu LG, Wang YY, Han KJ, Li LY, Zhai Z et al. (2005) VISA is an adapter protein required for virus-triggered IFN-beta signaling. Mol Cell 19: 727-740. doi:10.1016/j.molcel.2005.08.014. PubMed: 16153868.
4. Seth RB, Sun L, Ea CK, Chen ZJ (2005) Identification and characterization of MAVS, a mitochondrial antiviral signaling protein that activates NF-kappaB and IRF 3. Cell 122: 669-682. doi:10.1016/j.cell.2005.08.012. PubMed: 16125763.
5. Meylan E, Curran J, Hofmann K, Moradpour D, Binder M et al. (2005) Cardif is an adaptor protein in the RIG-I antiviral pathway and is targeted by hepatitis C virus. Nature 437: 1167-1172. doi:10.1038/nature04193. PubMed: 16177806.
6. Kawai T, Takahashi K, Sato S, Coban C, Kumar H et al. (2005) IPS-1, an adaptor triggering RIG-I- and Mda5-mediated type I interferon induction. Nat Immunol 6: 981-988. doi:10.1038/ni1243. PubMed: 16127453.
7. Dixit E, Boulant S, Zhang Y, Lee AS, Odendall C et al. (2010) Peroxisomes are signaling platforms for antiviral innate immunity. Cell 141: 668-681. doi:10.1016/j.cell.2010.04.018. PubMed: 20451243.
8. Horner SM, Liu HM, Park HS, Briley J, Gale M Jr. (2011) Mitochondrial-associated endoplasmic reticulum membranes (MAM) form innate immune synapses and are targeted by hepatitis C virus. Proc Natl Acad Sci U S A 108: 14590-14595. doi:10.1073/pnas.1110133108. PubMed: 21844353.
9. Onoguchi K, Onomoto K, Takamatsu S, Jogi M, Takemura A et al. (2010) Virus-infection or 5'ppp-RNA activates antiviral signal through redistribution of IPS-1 mediated by MFN1. PLoS Pathog 6: e1001012. PubMed: 20661427.
10. Yasukawa K, Oshiumi H, Takeda M, Ishihara N, Yanagi Y et al. (2009) Mitofusin 2 inhibits mitochondrial antiviral signaling. Sci Signal 2: ra47. PubMed: 19690333.
11. Hou F, Sun L, Zheng H, Skaug B, Jiang QX et al. (2011) MAVS forms functional prion-like aggregates to activate and propagate antiviral innate immune response. Cell 146: 448-461. doi:10.1016/j.cell.2011.06.041. PubMed: 21782231.
12. Perry AK, Chow EK, Goodnough JB, Yeh WC, Cheng G (2004) Differential requirement for TANK-binding kinase-1 in type I interferon responses to toll-like receptor activation and viral infection. J Exp Med 199: 1651-1658. doi:10.1084/jem.20040528. PubMed: 15210743.
13. Hemmi H, Takeuchi O, Sato S, Yamamoto M, Kaisho T et al. (2004) The roles of two IkappaB kinase-related kinases in lipopolysaccharide and double stranded RNA signaling and viral infection. J Exp Med 199: 1641-1650. doi:10.1084/jem.20040520. PubMed: 15210742.
14. Oshiumi H, Matsumoto M, Funami K, Akazawa T, Seya T (2003) TICAM-1, an adaptor molecule that participates in Toll-like receptor 3-mediated interferon-beta induction. Nat Immunol 4: 161-167. doi:10.1038/ni886. PubMed: 12539043.
15. Matsumoto M, Funami K, Tanabe M, Oshiumi H, Shingai M et al. (2003) Subcellular localization of Toll-like receptor 3 in human dendritic cells. J Immunol 171: 3154-3162. PubMed: 12960343.
16. Alexopoulou L, Holt AC, Medzhitov R, Flavell RA (2001) Recognition of double-stranded RNA and activation of NF-kappaB by Toll-like receptor 3. Nature 413: 732-738. doi:10.1038/35099560. PubMed: 11607032.
17. Sun L, Wu J, Du F, Chen X, Chen ZJ (2013) Cyclic GMP-AMP synthase is a cytosolic DNA sensor that activates the type I interferon pathway. Science 339: 786-791. doi:10.1126/science.1232458. PubMed: 23258413.
18. Kondo T, Kobayashi J, Saitoh T, Maruyama K, Ishii KJ et al. (2013) DNA damage sensor MRE11 recognizes cytosolic double-stranded DNA and induces type I interferon by regulating STING trafficking. Proc Natl Acad Sci U S A 110: 2969-2974. doi:10.1073/pnas.1222694110. PubMed: 23388631.
19. Desmet CJ, Ishii KJ (2012) Nucleic acid sensing at the interface between innate and adaptive immunity in vaccination. Nat Rev Immunol 12: 479-491. doi:10.1038/nri3247. PubMed: 22728526.
20. Stetson DB, Medzhitov R (2006) Recognition of cytosolic DNA activates an IRF3-dependent innate immune response. Immunity 24: 93-103. doi:10.1016/j.immuni.2005.12.003. PubMed: 16413926.
21. Ishii KJ, Coban C, Kato H, Takahashi K, Torii Y et al. (2006) A Toll-like receptor-independent antiviral response induced by double-stranded B-form. DNA - Nat Immunol 7: 40-48. doi:10.1038/ni1282.
22. Choi MK, Wang Z, Ban T, Yanai H, Lu Y et al. (2009) A selective contribution of the RIG-I-like receptor pathway to type I interferon responses activated by cytosolic. DNA - Proc Natl Acad Sci U S A 106: 17870-17875. doi:10.1073/pnas.0909545106.
23. Cheng G, Zhong J, Chung J, Chisari FV (2007) Double-stranded DNA and double-stranded RNA induce a common antiviral signaling pathway in human cells. Proc Natl Acad Sci U S A 104: 9035-9040. doi:10.1073/pnas.0703285104. PubMed: 17517627.
24. Chiu YH, Macmillan JB, Chen ZJ (2009) RNA polymerase III detects cytosolic DNA and induces type I interferons through the RIG-I pathway. Cell 138: 576-591. doi:10.1016/j.cell.2009.06.015. PubMed: 19631370.
25. Ishikawa H, Ma Z, Barber GN (2009) STING regulates intracellular DNA-mediated, type I interferon-dependent innate immunity. Nature 461: 788-792. doi:10.1038/nature08476. PubMed: 19776740.
26. Ishikawa H, Barber GN (2008) STING is an endoplasmic reticulum adaptor that facilitates innate immune signalling. Nature 455: 674-678. doi:10.1038/nature07317. PubMed: 18724357.
27. Ishii KJ, Kawagoe T, Koyama S, Matsui K, Kumar H et al. (2008) TANK-binding kinase-1 delineates innate and adaptive immune responses to DNA vaccines. Nature 451: 725-729. doi:10.1038/nature06537. PubMed: 18256672.
28. Soulat D, Bürckstümmer T, Westermayer S, Goncalves A, Bauch A et al. (2008) The DEAD-box helicase DDX3X is a critical component of the TANK-binding kinase 1-dependent innate immune response. EMBO J 27: 2135-2146. doi:10.1038/emboj.2008.126. PubMed: 18583960.
29. Fitzgerald KA, McWhirter SM, Faia KL, Rowe DC, Latz E et al. (2003) IKKepsilon and TBK1 are essential components of the IRF3 signaling pathway. Nat Immunol 4: 491-496. doi:10.1038/ni921. PubMed: 12692549.

30. Oshiumi H, Miyashita M, Matsumoto M, Seya T (2013) A Distinct Role of Riplet-Mediated K63-Linked Polyubiquitination of the RIG-I Repressor Domain in Human Antiviral Innate Immune Responses. PLOS Pathog 9: e1003533.
31. Yoneyama M, Kikuchi M, Natsukawa T, Shinobu N, Imaizumi T et al. (2004) The RNA helicase RIG-I has an essential function in double-stranded RNA-induced innate antiviral responses. Nat Immunol 5: 730-737. doi:10.1038/ni1087. PubMed: 15208624.
32. Takaoka A, Wang Z, Choi MK, Yanai H, Negishi H et al. (2007) DAI (DLM-1/ZBP1) is a cytosolic DNA sensor and an activator of innate immune response. Nature 448: 501-505. doi:10.1038/nature06013. PubMed: 17618271.
33. Kumar H, Kawai T, Kato H, Sato S, Takahashi K et al. (2006) Essential role of IPS-1 in innate immune responses against RNA viruses. J Exp Med 203: 1795-1803. doi:10.1084/jem.20060792. PubMed: 16785313.
34. Aly HH, Oshiumi H, Shime H, Matsumoto M, Wakita T et al. (2011) Development of mouse hepatocyte lines permissive for hepatitis C virus (HCV). PLOS ONE 6: e21284. doi:10.1371/journal.pone.0021284. PubMed: 21731692.
35. Taketomi M, Nishi Y, Ohkawa Y, Inui N (1986) Establishment of lung fibroblastic cell lines from a non-human primate Tupaia belangeri and their use in a forward gene mutation assay at the hypoxanthine-guanine phosphoribosyl transferase locus. Mutagenesis 1: 359-365. doi:10.1093/mutage/1.5.359. PubMed: 3331674.
36. Kumar M, Jung SY, Hodgson AJ, Madden CR, Qin J et al. (2011) Hepatitis B virus regulatory HBx protein binds to adaptor protein IPS-1 and inhibits the activation of beta interferon. J Virol 85: 987-995. doi: 10.1128/JVI.01825-10. PubMed: 21068253.
37. Wang Z, Choi MK, Ban T, Yanai H, Negishi H et al. (2008) Regulation of innate immune responses by DAI (DLM-1/ZBP1) and other DNA-sensing molecules. Proc Natl Acad Sci U S A 105: 5477-5482. doi: 10.1073/pnas.0801295105. PubMed: 18375758.
38. Paludan SR, Bowie AG (2013) Immune sensing of DNA. Immunity 38: 870-880. doi:10.1016/j.immuni.2013.05.004. PubMed: 23706668.
39. Li XD, Wu J, Gao D, Wang H, Sun L et al. (2013) Pivotal roles of cGAS-cGAMP signaling in antiviral defense and immune adjuvant effects. Science 341: 1390-1394. doi:10.1126/science.1244040. PubMed: 23989956.
40. Oshiumi H, Matsumoto M, Hatakeyama S, Seya T (2009) Riplet/RNF135, a RING finger protein, ubiquitinates RIG-I to promote interferon-beta induction during the early phase of viral infection. J Biol Chem 284: 807-817. PubMed: 19017631.
41. Oshiumi H, Miyashita M, Inoue N, Okabe M, Matsumoto M et al. (2010) The ubiquitin ligase Riplet is essential for RIG-I-dependent innate immune responses to RNA virus infection. Cell Host Microbe 8: 496-509. doi:10.1016/j.chom.2010.11.008. PubMed: 21147464.

Molecular Immunology 57 (2014) 100–110

Contents lists available at ScienceDirect

Molecular Immunology

journal homepage: www.elsevier.com/locate/molimm

MAVS-dependent IRF3/7 bypass of interferon β-induction restricts the response to measles infection in CD150Tg mouse bone marrow-derived dendritic cells

Hiromi Takaki[a], Kenya Honda[b], Koji Atarashi[b], Fukiko Kobayashi[a], Takashi Ebihara[a,1], Hiroyuki Oshiumi[a], Misako Matsumoto[a], Masashi Shingai[a,2], Tsukasa Seya[a,*]

[a] Department of Microbiology and Immunology, Graduate School of Medicine, Hokkaido University, Kita-ku, Sapporo 060-8638, Japan
[b] Laboratory for Gut Homeostasis, RIKEN Center for Integrative Medical Sciences, 1-7-22 Suehiro-cho, Tsurumi-ku, Yokohama, Kanagawa 230-0045, Japan

ARTICLE INFO

Article history:
Received 7 June 2013
Received in revised form 7 August 2013
Accepted 15 August 2013

Keywords:
Innate immunity
Dendritic cells
Type I interferon
Mitochondrial antiviral signaling protein (MAVS)
Measles virus

ABSTRACT

Measles virus (MV) infects CD150Tg/*Ifnar* (IFN alpha receptor)$^{-/-}$ mice but not CD150 (a human MV receptor)-transgenic (Tg) mice. We have shown that bone marrow-derived dendritic cells (BMDCs) from CD150Tg/*Ifnar*$^{-/-}$ mice are permissive to MV in contrast to those from simple CD150Tg mice, which reveals a crucial role of type I interferon (IFN) in natural tropism against MV. Yet, the mechanism whereby BMDCs produce initial type I IFN has not been elucidated in MV infection. RNA virus infection usually allows cells to generate double-stranded RNA and induce activation of IFN regulatory factor (IRF) 3/7 transcription factors, leading to the production of type I IFN through the retinoic acid-inducible gene I (RIG-I)/melanoma differentiation-associated gene 5 (MDA5)-mitochondrial antiviral signaling protein (MAVS) pathway. In mouse experimental BMDCs models, we found CD150Tg/*Mavs*$^{-/-}$BMDCs, but not CD150Tg/*Irf3*$^{-/-}$/*Irf7*$^{-/-}$BMDCs, permissive to MV. IFN-α/β were not induced in MV-infected CD150Tg/*Mavs*$^{-/-}$BMDCs, while IFN-β was subtly induced in CD150Tg/*Irf3*$^{-/-}$/*Irf7*$^{-/-}$BMDCs. *In vivo* systemic infection was therefore established by transfer of MV-infected CD150Tg/*Mavs*$^{-/-}$ BMDCs to CD150Tg/*Ifnar*$^{-/-}$ mice. These data indicate that MAVS-dependent, IRF3/7-independent IFN-β induction triggers the activation of the IFNAR pathway so as to restrict the spread of MV by infected BMDCs. Hence, MAVS participates in the initial induction of type I IFN in BMDCs and IFNAR protects against MV spreading. We also showed the importance of IL-10-producing CD4^{+} T cells induced by MV-infected BMDCs *in vitro*, which may account for immune modulation due to the functional aberration of DCs.

1. Introduction

Recognition of viral RNA in infected cells results in activation of IRF and induction of type I IFN, which initiates potent antiviral responses (Honda et al., 2006; Rathinam and Fitzgerald, 2011). RIG-I and MDA5 sense cytoplasmic viral RNA to activate IRF3/7 through the adaptor MAVS, while TLR3 recognizes extracellular RNA to signal IRF3/7 through the adaptor TICAM-1 (Kawai and Akira, 2006; Matsumoto et al., 2011). Each virus species has its own strategy to circumvent IFN induction, thereby successfully replicating in host cells.

MV is a negative-strand RNA virus, that infects human cells and rapidly induces a Th1 response in children which is characterized by high levels of IFN-γ and IL-2 in the early phase (Griffin et al., 1990). Paradoxically, MV infection is also accompanied by a severe suppression of the immune response that may last for months and this increases the vulnerability to secondary life-threatening infections (Schneider-Schaulies et al., 1995; Moss et al., 2004). Although consensus conclusions are limited in this issue, host dendritic cells (DCs) and acute type I IFN/IL-10 responses are critically implicated in a MV-mediated immune modulation.

It has been reported that V protein of MV wild-type strains blocks IFN-inducing signaling, thereby most wild-type strains can replicate in human cells without interfering with type I IFN

Abbreviations: BM, bone marrow; MAVS, mitochondrial antiviral signaling protein; MDA5, melanoma differentiation associated gene 5; MV, measles virus; RIG-I, retinoic acid inducible gene-I; TICAM1, Toll/IL-1 receptor homology domain-containing adaptor molecule 1; WT, wild-type.

* Corresponding author at: Department of Microbiology and Immunology, Hokkaido University, Graduate School of Medicine, Kita 15, Nishi 7, Kita-ku, Sapporo 060-8638, Japan. Tel.: +81 11 706 7866; fax: +81 11 706 7866.
E-mail address: seya-tu@pop.med.hokudai.ac.jp (T. Seya).
[1] Present address: Howard Hughes Medical Institute, Rheumatology Division, Department of Medicine, Campus Box 8045, Washington University Medical Center, 660 South Euclid Avenue, St Louis, MO 63110-1093, USA.
[2] Present address: Laboratory of Molecular Microbiology, National Institute of Allergy and Infectious Diseases, National Institutes of Health, Bethesda, MD 20892, USA.

0161-5890/$ – see front matter © 2013 Elsevier Ltd. All rights reserved.
http://dx.doi.org/10.1016/j.molimm.2013.08.007

(Takeuchi et al., 2003; Shingai et al., 2007; Ikegame et al., 2010). Several laboratory-adapted strains of MV which produce defective interfering (DI) RNA (Shingai et al., 2007), and a rescued strain called Edmonston tag (Radecke et al., 1995) that harbors C272R-mutated V protein (Ohno et al., 2004), induces type I IFN and explains the mechanism of IFN induction by this MV clone (Takaki et al., 2011). Cytoplasmic RNA sensors, RIG-I and MDA5, are involved in MV RNA recognition and following type I IFN induction (Ikegame et al., 2010), that causes IFNAR-mediated amplification (Takeuchi et al., 2003). RIG-I and MDA5 deliver signals through mitochondrial antiviral signaling protein (MAVS, also called IPS-1/Cardif/VISA) (Yoneyama et al., 2008). Minimal participation of TLRs in MV replication has been reported in human cells including macrophages and dendritic cells (Murabayashi et al., 2002; Tanabe et al., 2003).

The dsRNA-sensing system is believed to be essentially the same in the human and mouse, except that the type I IFN basal level is relatively high in the intact mouse (Shingai et al., 2005). We have made mouse models for analysis of immune aberration induced by various virus infections (Matsumoto et al., 2011). Human CD150 is a main entry receptor for MV, and expressed on DCs, macrophages, T and B cells, (Tatsuo et al., 2000). *Ifnar*$^{-/-}$ mice with transgenic human CD150 (CD150Tg/*Ifnar*$^{-/-}$) have been used as a MV infection model mouse (Welstead et al., 2005; Shingai et al., 2005; Sellin et al., 2009; Koga et al., 2010) and shown that bone marrow-derived (BM)DCs are highly susceptible to MV (Shingai et al., 2005) as in human monocyte-derived or CD34$^+$ progenitor-derived DCs (Fugier-Vivier et al., 1997; Grosjean et al., 1997). Actually, transfer of MV-infected BMDCs to CD150Tg/*Ifnar*$^{-/-}$ mice facilitates establishing systemic MV infection in mice (Shingai et al., 2005).

Here, we generated CD150Tg/*Mavs*$^{-/-}$, CD150Tg/*Irf3*$^{-/-}$/*Irf7*$^{-/-}$, and CD150Tg/*Ticam1*$^{-/-}$ mouse sublines and compared the MV-permissiveness of their BMDCs to those of BMDCs from CD150Tg/*Ifnar*$^{-/-}$ mice by *in vitro* MV infection and *in vivo* BMDC-transfer analyses. We found that the IFN response initially elicited by MV was abolished in CD150Tg/*Mavs*$^{-/-}$ BMDCs, but not CD150Tg/*Irf3*$^{-/-}$/*Irf7*$^{-/-}$ BMDCs, and therefore CD150Tg/*Mavs*$^{-/-}$ BMDCs are permissive to MV infection, similar to CD150Tg/*Ifnar*$^{-/-}$ BMDCs. We report here the results of an analysis of CD150Tg/*Mavs*$^{-/-}$ BMDCs in MV infection. Moreover, we show that MV-infected BMDCs induce the differentiation of naïve CD4$^+$ T cells into high levels of IL-10- and IFN-γ-producing T cells.

2. Materials and methods

2.1. Mice

All knockout mice were backcrossed with C57BL/6 mice more than eight times before use. CD150Tg (Shinagi et al., 2005), *Ticam1*$^{-/-}$ (Akazawa et al., 2007) and *Mavs*$^{-/-}$ (Oshiumi et al., 2011) mice were generated in our laboratory. *Irf3*$^{-/-}$/*Irf7*$^{-/-}$ double knockout (DKO) mice (Sato et al., 2000) and IL-10 Venus mice (Atarashi et al., 2011) were provided by Dr. T. Taniguchi (University of Tokyo, Tokyo, Japan) and Dr. K. Honda (RIKEN Research Center for Allergy and Immunology), respectively. This study was carried out in strict accordance with the recommendations in the Guide for the Care and Use of Laboratory Animals of the National Institutes of Health. The protocol was approved by the Committee on the Ethics of Animal Experiments in the Animal Safety Center, Hokkaido University, Japan. All mice were used according to the guidelines of the Institutional Animal Care and Use Committee of Hokkaido University, who approved this study as no.08-0244. All inoculation and experimental manipulation was performed under anesthesia that was induced and maintained with pentobarbital sodium, and all efforts were made to minimize suffering. All mice were maintained under specific pathogen-free conditions in the Animal Facility at Hokkaido University Graduate School of Medicine (Sapporo, Japan) and used when they were between 6 and 12 weeks of age.

2.2. Cell culture

Vero/CD150 cells were maintained in DMEM supplemented with 10% heat-inactivated FBS and antibiotics. BMDCs were generated from bone marrow according to the method described by Inaba et al. (1992), with slight modifications. Briefly, bone marrow samples from the femurs and tibiae of mice were cultured in RPMI 1640 (GIBCO) with 10% heat-inactivated FBS containing GM-CSF (J558 supernatant) for 6 days with replenishment of the medium every other day. Splenic naïve CD4$^+$ CD25$^-$ T cells were isolated by negative selection using the biotin-CD8a, CD11b, B220, Dx5, Gr1, CD25 anitbody and streptavidin beads (Miltenyi Biotec) (typically >90% purity) (Akazawa et al., 2007). For coculture experiment, 2×10^5 CD4$^+$ T cells and 1×10^4 mock or with MV-infected BMDCs were cocultured with or without anti-CD3 antibody (0.1 μg/ml) for 4 or 6 days. For restimulation, 4×10^5 CD4$^+$ T cells were cultured with the plate bound anti-CD3 antibody (0–1 μg/ml) for 48 h.

2.3. Virus

IC323, corresponding to the IC-B strain of MV was recovered from the plasmid p(+)MV323 encoding the antigenomic IC-B sequence (Takeda et al., 2000). IC323-Luci (MV-luciferase) was kindly gifted from Dr. M. Takeda (Department of Virology III, National Institute of Infectious Disease, Tokyo, Japan) (Takeda et al., 2007). MV-luciferase and MV-GFP (Shingai et al., 2005) were maintained in Vero/CD150 cells (Shingai et al., 2007). Virus titer was determined as plaque forming units (PFUs) on Vero/CD150 cells and the MOI of each experiment was calculated based on this titer (Kobune et al., 1990). To measure the efficiency of *in vitro* infection, cells (5×10^4 to 2×10^5) were harvested in 25 μl of lysis buffer for luciferase assays. Luciferase assays were performed using a Dual-Luciferase reporter assay system (Promega), and luciferase activity was read using Lumat LB 9507 (Berthold Technologies). Luciferase activity is shown as means ± S.D. of three samples.

2.4. In vivo infection and BMDCs transfer

Six- to 12-week-old mice were used throughout this study. Mice were infected i.p. with MV-GFP at dose of 1×10^6 pfu. At 3 and 6 days after inoculation, sera were collected from MV- or mock-infected mice. At 4 days after inoculation, CD4$^+$ cells, CD8$^+$ cells, CD11c$^+$ cells and CD19$^+$ cells were isolated from splenocytes of MV or mock infected mice using anti-CD4, anti-CD8, anti-CD11c and anti-CD19 MACS beads (Miltenyi Biotec). The purity of isolated cells was >90%. For BMDCs transfer, CD150Tg/*Mavs*$^{-/-}$ BMDCs were infected with MV (MOI = 0.25) or mock for 24 h. BMDCs were washed 4 times and resuspended with PBS. Cells (1×10^6 cells) were intravenously transferred to CD150Tg, CD150Tg/*Ifnar*$^{-/-}$ and CD150Tg/*Mavs*$^{-/-}$ mice. After 4 days, splenocytes (1×10^7 cells) and LNs (1×10^7 cells) were collected and CD4$^+$ cells, CD8$^+$ cells, CD11c$^+$ cells and CD19$^+$ cells were isolated from the splenocytes. MV titers in these cells were determined by measuring luciferase activity.

2.5. ELISA

Culture supernatants of cells ($3–5 \times 10^5$) seeded on 24-well plates were collected and analyzed for cytokine levels with enzyme-linked immunosorbent assay (ELISA). ELISA kits for mouse IFN-α and IFN-β were purchased from PBL Biomedical Laboratories. ELISA kits for mouse IL-10, IL-13 and IFN-γ were purchased from

eBiosciences. ELISA was performed according to the manufacturer's instructions.

2.6. RT-PCR and real-time PCR

Total RNA was prepared using TRIzol Reagent (Invitrogen) following the manufacturer's instructions. RT-PCR was carried out using the High Capacity cDNA Reverse Transcripition kit (Applied Biosystems) according to the manufacturer's instructions. The nucleotide sequences of the primers for real-time PCR are shown in Supplemental Table I. Real-time PCR was performed using a Step One real-time PCR system (Applied Biosystems). Expression levels of target mRNA were normalized to *β-actin* and fold inductions of transcripts were calculated using the ddCT method relative to unstimulated cells.

Supplementary data associated with this article can be found, in the online version, at http://dx.doi.org/10.1016/j.molimm.2013.08.007.

2.7. FACS analysis

BMDCs were stained with anti-CD11c-APC (eBiosciences) and anti-human CD150-FITC (eBiosciences) and fluorescence intensity was measured by FACS Calibur. For Foxp3 intracellular staining, cells were stained with anti-CD25-PE (eBiosciences), anti-CD4-FITC (eBiosciences) and anti-Foxp3-APC using Foxp3 staining kit (eBiosciences). For IFN-γ intracellular staining, cells were stained with anti-IFN-γ-APC using BD Cytofix/Cytoperm kit (BD Biosciences). Stained cells were analyzed by flow cytometry.

2.8. Statistical analyses

Statistical significance of differences between groups was determined by the Student *t* test using Microsoft Excel software. Values of $p < 0.05$ were considered significant.

3. Results

3.1. CD150Tg/Mavs$^{-/-}$ BMDCs were permissive to MV infection

To identify the induction pathway for the type I IFN response to MV infection, we crossed CD150Tg mice with *Irf3*$^{-/-}$/*Irf7*$^{-/-}$, *Ticam1*$^{-/-}$ and *Mavs*$^{-/-}$ mice. First, we measured the expression levels of human CD150 in BMDCs derived from the CD150Tg, CD150Tg/*Ifnar*$^{-/-}$, CD150Tg/*Irf3*$^{-/-}$/*Irf7*$^{-/-}$, CD150Tg/*Ticam1*$^{-/-}$ and CD150Tg/*Mavs*$^{-/-}$ mice using FACS analysis (Fig. 1A). The expression levels of human CD150 were not changed in the BMDCs from any of the CD150Tg/*Ifnar*$^{-/-}$, CD150Tg/*Irf3*$^{-/-}$/*Irf7*$^{-/-}$, CD150Tg/*Ticam1*$^{-/-}$ and CD150Tg/*Mavs*$^{-/-}$ mice (Fig. 1A). In all of the different BMDC genotypes used in this study, human CD150 expression was upregulated in response to LPS and PolyI:C and downregulated by infection with live MV and heated MV (Supplemental Fig. 1). BMDCs were infected with MV-GFP at MOI of 0.25 for 24 h and the percentage of GFP$^+$ cells was determined by FACS analysis. While CD150Tg BMDCs were barely permissive to MV compared to mock, ~5% of the CD11c$^+$ BMDCs derived from the CD150Tg/*Ifnar*$^{-/-}$ mice were infected (Fig. 1B). We expected that CD150Tg/*Irf3*$^{-/-}$/*Irf7*$^{-/-}$ BMDCs would be permissive to MV infection, because IRF3 and IRF7 are essential molecules for type I IFN induction in response to viral infection (Sato et al., 2000). However, MV only marginally infected the BMDCs derived from the CD150Tg/*Irf3*$^{-/-}$/*Irf7*$^{-/-}$ mice (Fig. 1B). The CD150Tg/*Ticam1*$^{-/-}$ BMDCs were hardly as permissive to MV as CD150Tg BMDCs (Fig. 1B). Approximately 6% of CD150Tg/*Mavs*$^{-/-}$ BMDCs were infected with MV and the infection efficiency in CD150Tg/*Mavs*$^{-/-}$ BMDCs was comparable to that in CD150Tg/*Ifnar*$^{-/-}$ BMDCs (Fig. 1B). A previous report suggested that the IFN-inducing pathway in CD11c$^+$ BMDCs is critically implicated in establishment of MV infection (Shingai et al., 2005). Here, we show the molecular evidence that MAVS and IFNAR are crucial for protection against MV.

Supplementary data associated with this article can be found, in the online version, at http://dx.doi.org/10.1016/j.molimm.2013.08.007.

To confirm the efficiency of MV-GFP infection in BMDCs, we used a recombinant MV-luciferase which encodes the reporter *Renilla* luciferase (Takeda et al., 2007). Luciferase activity obtained from MV-infected Vero cells was correlated with the viral titer of MV-infected cells (Supplemental Fig. 2). BMDCs were infected with MV-luciferase at MOI of 0.25 for 24 h and luciferase activity was measured (Fig. 1C). As similar to the results from MV-GFP infection, CD150Tg, and CD150Tg/*Ticam1*$^{-/-}$ BMDCs were not permissive to MV infection compared with CD150Tg/*Ifnar*$^{-/-}$ BMDCs. On the other hand, a subtle increase of luciferase activity was observed in CD150Tg/*Irf3*$^{-/-}$/*Irf7*$^{-/-}$ BMDCs. Furthermore, the luciferase activity levels obtained from MV-infected CD150Tg/*Ifnar*$^{-/-}$ and CD150Tg/*Mavs*$^{-/-}$ BMDCs were approximately 2-fold higher than those in CD150Tg BMDCs (Fig. 1C). These data suggest that the loss of MAVS rather than IRF3/7 critically determines MV-permissiveness in CD150Tg BMDCs: *i.e.* an additional transcription factor other than IRF3/7 participates in the protection of CD150Tg BMDCs from MV infection *in vitro*.

Supplementary data associated with this article can be found, in the online version, at http://dx.doi.org/10.1016/j.molimm.2013.08.007.

3.2. Type I IFN induction rendered CD150Tg/Irf3$^{-/-}$/Irf77$^{-/-}$ BMDCs MV-nonpermissive

Next, to clarify the reason why MV was barely able to infect CD150Tg/*Irf3*$^{-/-}$/*Irf7*$^{-/-}$BMDCs, we evaluated type I IFN expression in MV-infected BMDCs (Fig. 2A). As expected, *Ifn-α4* mRNA was induced by MV infection in CD150Tg, CD150Tg/*Ifnar*$^{-/-}$ and CD150Tg/*Ticam1*$^{-/-}$BMDCs, but not in CD150Tg/*Irf3*$^{-/-}$/*Irf7*$^{-/-}$ or CD150Tg/*Mavs*$^{-/-}$BMDCs (Fig. 2A). IFN-α protein was also induced in CD150Tg, CD150Tg/*Ticam1*$^{-/-}$BMDCs and to a lesser extent in CD150Tg/*Ifnar*$^{-/-}$ BMDCs (Fig. 2B). The message-protein discrepancy was observed with IFN-α4 in MV-infected CD150Tg/*Ifnar*$^{-/-}$ mice as reported (Marié et al., 1998). In contrast, *Ifn-β* mRNA expression was observed in CD150Tg, CD150Tg/*Ifnar*$^{-/-}$, CD150Tg/*Ticam1*$^{-/-}$BMDCs and CD150Tg/*Irf3*$^{-/-}$/*Irf7*$^{-/-}$BMDCs (Fig. 2A). *Ifn-β* was barely detected in CD150Tg/*Mavs*$^{-/-}$BMDCs. We confirmed the production of the IFN-β protein from MV-infected CD150Tg/*Irf3*$^{-/-}$/*Irf7*$^{-/-}$ BMDCs using ELISA, and found the protein level of IFN-β slightly but firmly detected in the MV-infected *Irf3*$^{-/-}$/*Irf7*$^{-/-}$ BMDCs (Fig. 2B). This IRF3/IRF7-independent *Ifn-β* induction was almost completely abolished by an NF-κB inhibitor (BAY11-7082) but not ATF2 inhibitor (SB203580) (Supplemental Fig. 3). These data suggest that IFN-β, but not IFN-α, is induced in CD150Tg/*Irf3*$^{-/-}$/*Irf7*$^{-/-}$ BMDCs in response to MV infection, and then CD150Tg/*Irf3*$^{-/-}$/*Irf7*$^{-/-}$ BMDCs become relatively resistant to MV infection. To examine this possibility, BMDCs derived from mice of various genotypes were infected with MV in the presence of the anti-IFNAR antibody. As expected, MV infected CD150Tg/*Irf3*$^{-/-}$/*Irf7*$^{-/-}$ BMDCs in the presence of the anti-IFNAR antibody (Fig. 2C). The effect of the anti-IFNAR antibody on MV infection in CD150Tg/*Mavs*$^{-/-}$ BMDCs was weak (Fig. 2C). These results were confirmed by using MV-luciferase (Supplemental Fig. 4). These data suggest that MV infection induces IFN-β production in BMDCs in part independent of IRF3/IRF7. In contrast, due to the absence of IFN-α/β induction in the MV-infected CD150Tg/*Mavs*$^{-/-}$ BMDCs (Fig. 2A and B), MV

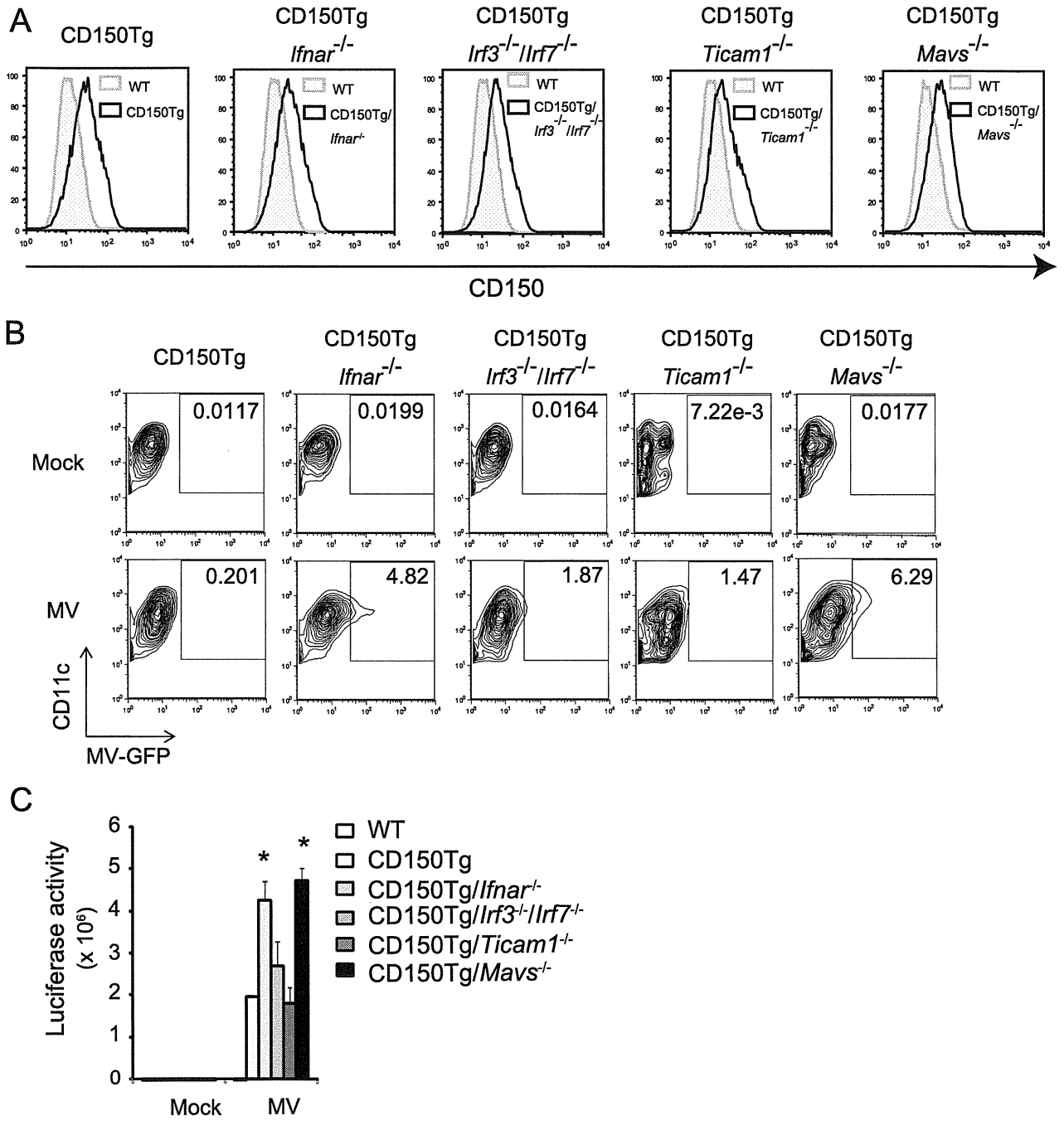

Fig. 1. CD150Tg/*Mavs*$^{-/-}$ BMDCs were permissive to MV infection. (A) Expression levels of human CD150 in BMDCs derived from WT, CD150Tg, CD150Tg/*Ifnar*$^{-/-}$, CD150Tg/*Irf3*$^{-/-}$/*Irf7*$^{-/-}$, CD150Tg/*Ticam1*$^{-/-}$ and CD150Tg/*Mavs*$^{-/-}$ mice were measured by FACS. The results are representative of three different experiments. (B) BMDCs generated from CD150Tg, CD150Tg/*Ifnar*$^{-/-}$, CD150Tg/*Irf3*$^{-/-}$/*Irf7*$^{-/-}$, CD150Tg/*Ticam1*$^{-/-}$ and CD150Tg/*Mavs*$^{-/-}$ mice were infected with MV-GFP (MOI = 0.25). At 24 h after infection, the efficiency of virus infection was evaluated by GFP expression using FACS. The numbers indicate the percentages of cells expressing GFP. The results are representative of three different experiments. (C) BMDCs derived from WT, CD150Tg, CD150Tg/*Ifnar*$^{-/-}$, CD150Tg/*Irf3*$^{-/-}$/*Irf7*$^{-/-}$, CD150Tg/*Ticam1*$^{-/-}$ and CD150Tg/*Mavs*$^{-/-}$ mice were infected with MV-luciferase (MOI = 0.25). At 24 h after infection, the luciferase activity in BMDCs was measured. The data are the means ± SD of three independent samples. *$p < 0.05$, MV-infected CD150Tg BMDCs vs. MV-infected knockout BMDCs.

was able to infect CD150Tg/*Mavs*$^{-/-}$ BMDCs. Moreover, type I IFN expression in response to MV infection depends on the MAVS pathway in BMDCs.

Supplementary data associated with this article can be found, in the online version, at http://dx.doi.org/10.1016/j.molimm.2013.08.007.

We next examined whether MV-infected CD150Tg/*Mavs*$^{-/-}$ BMDCs were able to transmit virus to lymphoid cells *in vivo*. CD150Tg/*Mavs*$^{-/-}$ BMDCs infected with MV-luciferase (MOI = 0.25) were intravenously transferred into CD150Tg, CD150Tg/*Ifnar*$^{-/-}$ and CD150Tg/*Mavs*$^{-/-}$ mice (Fig. 2D). After 4 days, the spleens and lymph nodes (LNs) were harvested and the MV luciferase activity was measured. Luciferase activity was not detected in CD150Tg splenocytes and LNs when mock-infected CD150Tg/*Mavs*$^{-/-}$ BMDCs were transferred. The luciferase activity in the spleen and LNs was increased when MV-infected CD150Tg/*Mavs*$^{-/-}$ BMDCs were transferred to CD150Tg mice (Fig. 2D). This result shows that MV-infected CD150Tg/*Mavs*$^{-/-}$ BMDCs transmit virus to spleen and LN cells in CD150Tg mice. The luciferase activity

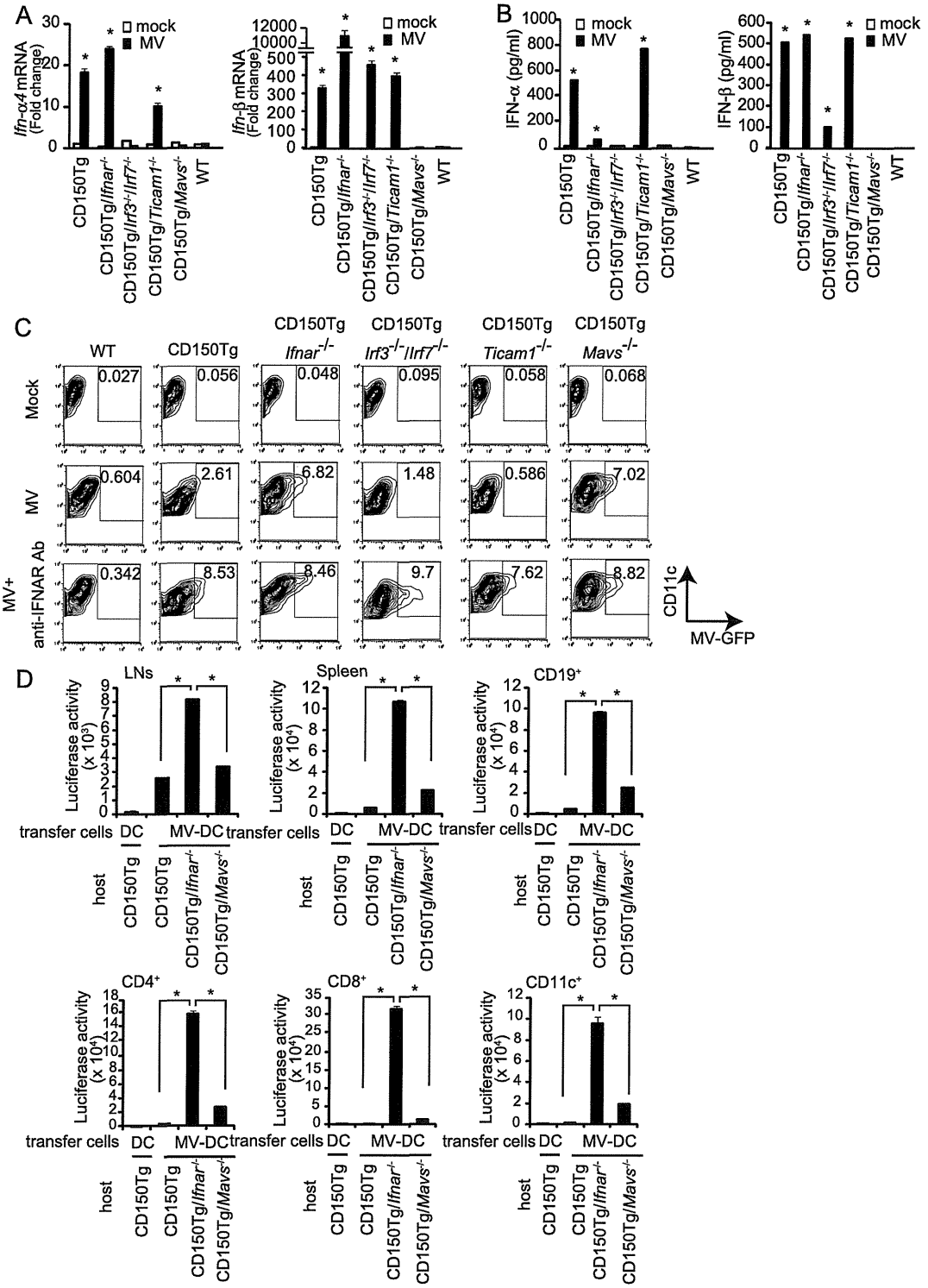

Fig. 2. MV infection did not induce type I IFN in CD150Tg/*Mavs*$^{-/-}$ BMDCs. BMDCs derived from WT, CD150Tg, CD150Tg/*Ifnar*$^{-/-}$, CD150Tg/*Irf3*$^{-/-}$/*Irf7*$^{-/-}$, CD150Tg/*Ticam1*$^{-/-}$ and CD150Tg/*Mavs*$^{-/-}$ mice were infected with MV-GFP (MOI = 0.25) or mock infected. (A) At 24 h after infection, *Ifn-α4* and *Ifn-β* mRNA expression was determined by real-time PCR. The data are the means ± SD of three independent samples. *$p < 0.05$, vs. mock-infected. (B) At 24 h after infection, IFN-α and IFN-β in the culture supernatants were measured by ELISA. The data are the means ± SD of three independent samples. * $p < 0.05$, vs. mock-infected. (C) BMDCs derived from WT, CD150Tg, CD150Tg/*Ifnar*$^{-/-}$, CD150Tg/*Irf3*$^{-/-}$/*Irf7*$^{-/-}$, CD150Tg/*Ticam1*$^{-/-}$ and CD150Tg/*Mavs*$^{-/-}$ mice were infected with MV-GFP (MOI = 0.25) or mock infected in the presence or absence of an anti-IFNAR antibody (10 μg/ml). At 24 h after infection, GFP expression was measured by FACS. The numbers shown are the percentages of cells expressing GFP. The results are representative of three different experiments. (D) BMDCs derived from CD150Tg/*Mavs*$^{-/-}$ mice were infected with MV-luciferase (MOI = 0.25) or mock infected for 24 h. BMDCs (1×10^6 cells) were washed 4 times and intravenously transferred to CD150Tg, CD150Tg/*Ifnar*$^{-/-}$ and CD150Tg/*Mavs*$^{-/-}$ mice. At 4 days after the transfer, splenocytes and LNs were collected and measured lucifrease activity. Luciferase activity was normalized by the total number of cells. Data are shown as the luciferase activity per 1×10^7 cells. The data are the means ± SD of three independent samples. * $p < 0.05$.

obtained from spleens and LNs of CD150Tg/*Ifnar*$^{-/-}$ mice with MV-infected BMDCs was much higher than CD150Tg mice. On the other hand, the efficiency of infection in the spleen and LNs of CD150Tg/*Mavs*$^{-/-}$ mice with MV-infected BMDCs was less than that for CD150Tg/IFNAR$^{-/-}$ mice. These results were confirmed with CD19$^+$, CD4$^+$, CD8$^+$ and CD11c$^+$ cells isolated from splenocytes (Fig. 2D). These results infer that the spread of MV infection is dependent on IFNAR rather than MAVS in host cells.

3.3. CD4$^+$ T cells produced IL-10 when CD4$^+$ T cells were cocultured with MV-infected BMDCs

Next, we focused on CD150Tg/*Ifnar*$^{-/-}$ cells because type I IFN induction in response to MV infection is known to be an important determinant of permissiveness to MV. MV infection reportedly induces immunosuppression in humans, non-human primates and mice (Schneider-Schaulies et al., 1995; Moss et al., 2004). DCs are thought to play a pivotal role in the pathogenesis of MV infection and elicit immunosuppressive effects during and after acute MV infection (Schneider-Schaulies et al., 2003; Servet-Delprat et al., 2003). Inducible regulatory T cells (iTreg) have also been reported to participate in immunosuppression during MV infection (Welstead et al., 2005). CD4$^+$ T cells prepared from MV-infected CD150Tg/*Ifnar*$^{-/-}$ mice produced the Th2 cytokines, IL-10 and IL-4, and the blocking of IL-10 ameliorated immunosuppression in the MV infected mice (Koga et al., 2010). Therefore, we examined whether MV-infected BMDCs affected Treg induction and the production of cytokines from CD4$^+$ T cells. MV-infected CD150Tg/*Ifnar*$^{-/-}$ BMDCs were cocultured with naïve CD4$^+$ T cells prepared from wild type (WT) mice for 6 days and then cells were subjected to intracellular staining with an anti-Foxp3 antibody, which is known to be a marker of Treg. Approximately 3% of the CD4$^+$ T cells expressed Foxp3, which was comparable to the percentage in naïve CD4$^+$ T cells cocultured with uninfected BMDCs (Fig. 3A). Population of CD25$^+$ T cells was increased when naïve T cells were cocultured with MV-infected BMDCs (Fig. 3A). A large amount of IL-10 was produced in the supernatant of naïve CD4$^+$ T cells cocultured with MV-infected BMDCs and the amount was markedly high compared to that in naïve CD4$^+$ T cells cocultured with uninfected BMDCs (Fig. 3B). Moreover, IL-10 production was dependent on anti-CD3 stimulation (Fig. 3B). IFN-γ, a Th1 cytokine, was also detected in the supernatant from naïve CD4$^+$ T cells cocultured with MV-infected BMDCs at a level that was comparable to that from naïve CD4$^+$ T cells cocultured with uninfected BMDCs (Fig. 3B). To confirm these data, we performed intracellular staining for IL-10 and IFN-γ using IL-10 reporter mice, in which a cassette containing an internal ribosomal entry site and Venus was inserted immediately before the polyadenylation signal of the *Il10* gene (referred to IL-10 Venus mice) (Atarashi et al., 2011). IL-10 Venus$^+$ CD4$^+$ T cells and IFN-γ$^+$ CD4$^+$ T cells were significantly increased when T cells were cocultured with MV-infected BMDCs (Fig. 3C). On the other hand, T cells cocultured with uninfected BMDCs expressed IFN-γ but not IL-10 Venus (Fig. 3C).

We further examined whether these CD4$^+$ T cells produced IL-10. BMDCs, either MV-infected or non-infected, were mixed with T cells in anti-CD3-coated wells (Kemper et al., 2003). After 4 days, BMDC/CD4$^+$ T-coculture cells were restimulated with plate-bound anti-CD3 antibody for 3 days and the amount of IL-10 and IFN-γ production from CD4$^+$ T cells was determined (Fig. 3D). CD4$^+$ T cells cocultured with MV-infected BMDCs produced high levels of IL-10 and IFN-γ in a manner that was dependent upon anti-CD3 stimulation (Fig. 3D). Without CD4$^+$ T cells, the IL-10 level in the MV-infected BMDCs was not increased compared to the mock-infected BMDCs (Supplemental Fig. 5). This result indicates that MV-infected BMDCs induce the differentiation of naïve CD4$^+$ T cells into IL-10- and IFN-γ-producing T cells. The expression level of *Gata3* mRNA, a master regulator of Th2, was increased when naïve CD4$^+$ T cells were cocultured with MV-infected BMDCs (Fig. 3E). *c-Maf* mRNA, a master regulator of Tr1, and *Rorgt* mRNA, a master regulator of Th17, and *Foxp3* mRNAs were decreased in CD4$^+$ T cells cocultured with BMDCs (Fig. 3E). The expression level of *T-bet* mRNA, a master regulator of Th1, was increased when naïve CD4$^+$ T cells were cocultured with BMDCs (Fig. 3E). Taken together, the results indicate that MV-infected BMDCs affect naïve CD4$^+$ T cells in such a manner as to induce IL-10- and IFN-γ-producing T cells without any induction of Treg. Although recent reports have demonstrated that IL-27 promotes IL-10 production by CD4$^+$ T cells (Stumhofer et al., 2007; Fitzgerald et al., 2007; Awasthi et al., 2007), in this setting, IL-27 only partially contributed to MV-induced IL-10 production (Supplemental Fig. 6).

Supplementary material related to this article found, in the online version, at http://dx.doi.org/10.1016/j.molimm.2013.08.007.

3.4. CD4$^+$ T cells produced IL-10 in response to MV infection

The IL-10 level in the serum prepared from MV-infected CD150Tg/*Ifnar*$^{-/-}$ mice was not different from the level in mock-infected mice (Fig. 4A). To identify cell types that produce IL-10, we isolated subsets of the splenocytes from MV- or mock-infected CD150Tg/*Ifnar*$^{-/-}$ mice and restimulated. When CD4$^+$ T cells were isolated from MV-infected CD150Tg/*Ifnar*$^{-/-}$ mice, CD4$^+$ T cells produced a large amount of IL-10 in response to an anti-CD3 antibody (Fig. 4B) (Kemper et al., 2003). CD8$^+$ T cells, CD11c$^+$ DCs and CD19$^+$ B cells did not produce any evident IL-10 even in the presence of the anti-CD3 antibody, LPS or PMA plus ionomycin, respectively. CD150Tg/*Ifnar*$^{-/-}$ and CD150Tg/IL-10 Venus/*Ifnar*$^{-/-}$ mice were infected with MV. Four days after inoculation, splenocytes were restimulated with PMA, ionomycin and brefeldin A for 6 h and subjected to FACS analysis. IL-10 Venus expression significantly induced in CD4$^+$ T cells but not CD8$^+$ T cells, CD11c$^+$ DCs nor CD19$^+$ B cells derived from MV-infected CD150Tg/IL-10 Venus/*Ifnar*$^{-/-}$ mice (Fig. 4C). Moreover, IL-10 producing CD4$^+$ T cells were different subsets from IFN-γ producing T cells (Fig. 4D).

4. Discussion

We have demonstrated that CD150Tg/*Mavs*$^{-/-}$ BMDCs were permissive to MV *in vitro*. MV infection did not induce the expression of type I IFN mRNA or protein in CD150Tg/*Mavs*$^{-/-}$ BMDCs. These data suggest that MV-derived primary type I IFN depends on the MAVS pathway in BMDCs, the result being consistent with the fact that CD11c$^+$ DCs are a primary target for replication of MV (Shingai et al., 2005).

Unexpectedly, MV infection minimally occurred in BMDCs prepared from CD150Tg/*Irf3*$^{-/-}$/*Irf7*$^{-/-}$ mice, because of their capacity to produce IFN-β. When anti-IFNAR antibody was present, MV was able to infect CD150Tg/*Irf3*$^{-/-}$/*Irf7*$^{-/-}$ BMDCs. Therefore, MV-induced type I IFN production depends on not only the primary MAVS-IRF3/7 pathway but also the amplifiable IFNAR pathway in BMDCs, and that unidentified transcription factors, rather than IRF3/IRF7, participate in the primary induction of IFN-β. TLR3 signals the presence of exogenous RNA *via* the TICAM-1 adaptor (Oshiumi et al., 2003). Although TLR3/TICAM-1 participate in BMDC maturation in response to cell-derived virus RNA in RNA virus infections (Ebihara et al., 2008; Oshiumi et al., 2011), this is not the case in MV infection.

Ifn-β is reportedly induced in conjunction with the activation of transcription factors, IRF3, IRF7, ATF-2/c-Jun and NF-κB

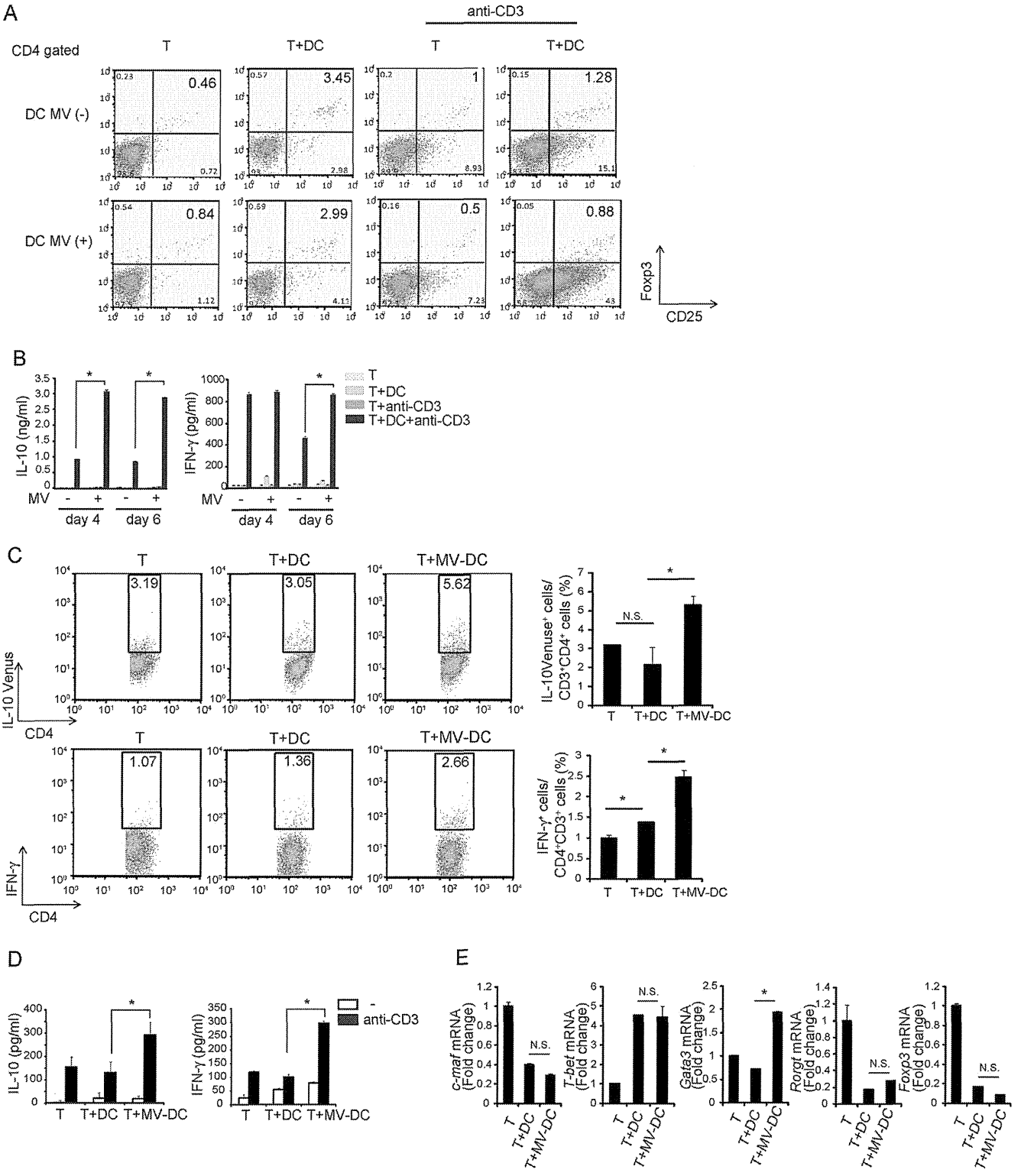

Fig. 3. MV-infected BMDCs induced IL-10 and IFN-γ producing CD4+ T cells. CD150Tg/*Ifnar*$^{-/-}$ BMDCs were infected with MV (MOI = 0.25) or mock for 24 h. Naïve CD4+CD25− T cells (2×10^5) isolated from WT mice were cocultured with 1×10^4 BMDCs in the presence or absence of 0.1 μg/ml of the anti-CD3 antibody. (A) At 6 days after coculture, cells were stained with anti-CD4, anti-CD25 and anti-Foxp3 antibodies and subjected to FACS analysis. The numbers shown are the percentage of CD25+Foxp3+ cells. The results are representative of three different experiments. (B) At 4 or 6 days after coculture, IL-10 and IFN-γ in the coculture supernatant were measured by ELISA. The data are the means ± SD of three independent samples. *$p < 0.05$. (C) CD4+ T cells isolated from IL-10 Venus mice were cocultured with uninfected or MV-infected CD150Tg/*Ifnar*$^{-/-}$ BMDCs for 4 days. Cells were stained with anti-CD3, anti-CD4 and anti-IFN-γ antibodies and analyzed by flow cytometry. The numbers shown are the percentage of CD4+IL-10 Venus+ cells and CD4+IFN-γ+ cells. The right graphs represent the fraction of the IL-10 Venus+ cell and IFN-γ+ cell populations. The data are the means ± SD of three independent samples. *$p < 0.05$. (D) At 4 days after the coculture, cells were collected and washed twice. Two x 10^5 cells were restimulated with the anti-CD3 plate-bound antibody for 3 days. At 3 days after restimulation, IL-10 and IFN-γ in the culture supernatants were measured by ELISA. The data are the means ± SD of three independent samples. *$p < 0.05$. (E). At 4 days after the cocultured, the expression level of *c-Maf*, *T-bet*, *Gata-3*, *Rorgt* and *Foxp3* mRNA in the CD4+ T cells cocultured with MV- or mock-infected BMDCs were determined by real-time PCR. The data are the means ± SD of three independent samples. N.S.; not significant, *$p < 0.05$.

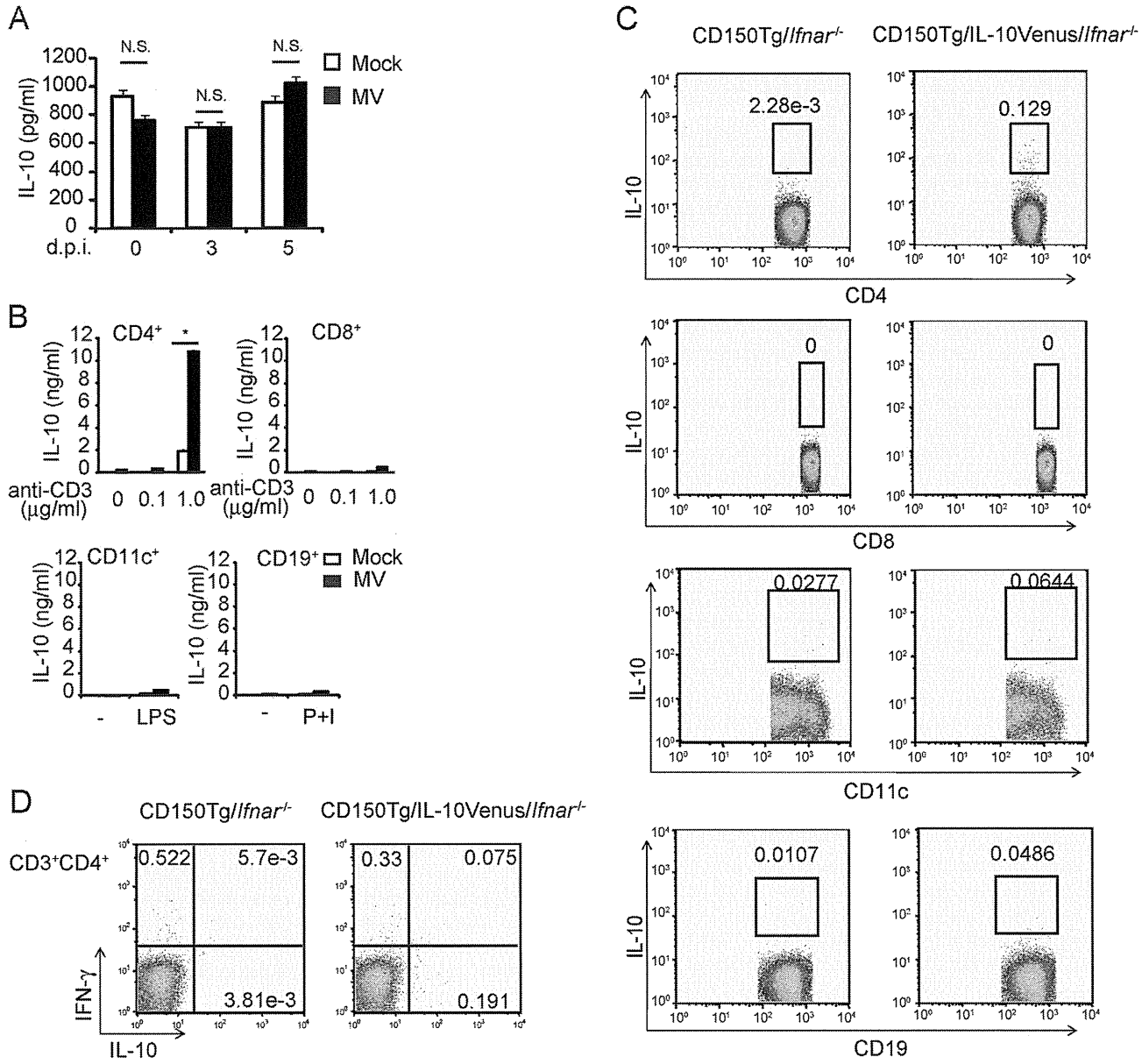

Fig. 4. CD4$^+$ T cells produced IL-10 *ex vivo*. (A) CD150Tg/*Ifnar*$^{-/-}$ mice were infected i.p. with 1×10^6 pfu MV-GFP or mock. At the indicated days after infection, IL-10 production in sera was measured by ELISA. The data are the means ± SD of three independent samples. N.S.; not significant. (B) CD150Tg/*Ifnar*$^{-/-}$ mice were infected i.p. with 1×10^6 pfu MV-GFP or mock infected. At 4 days after infection, CD4$^+$, CD8$^+$, CD11c$^+$ and CD19$^+$ cells were isolated from splenocytes and restimulated with plate-bound anti-CD3 (0–1.0 μg/ml), LPS (100 ng/ml) or PMA (1 μg/ml) plus ionomycin (1 μg/ml) (P+I), respectively. At 3 days after restimulation, IL-10 production in the culture supernatant was measured by ELISA. The data are the means ± SD of three independent samples. *$p < 0.05$. (C, D) CD150Tg/*Ifnar*$^{-/-}$ and CD150Tg/IL-10 Venus/*Ifnar*$^{-/-}$ mice were infected with MV (1×10^6 pfu). At 2 days after inoculation, splenocytes were stained with anti-CD3, anti-CD4, anti-CD8, anti-CD11c, anti-CD19, and anti-IFN-γ antibodies and subjected to FACS analysis. (C) The numbers shown are the percentage of IL-10$^+$ cells. (D) The numbers shown are the percentage of the gated populations. The results are representative of three different experiments.

(Thanos and Maniatis, 1995; Panne et al., 2007). The coordinated binding of these regulatory factors synergistically augments transcription of the *Ifn-β* gene in several different cell types (Thanos and Maniatis, 1995). MAVS-dependent IRF3/IRF7-bypassed *Ifn-β* induction has also been reported to take place through the NF-κB signaling pathway in West Nile virus infection, the case being not only for DCs (Daffis et al., 2009). Recently, the MAVS/IRF5-dependent pathway was identified to participate in type I IFN induction in West Nile virus-infected myeloid cells BMDCs (Lazear et al., 2013). IRF1 is also involved in TLR9-mediated IFN-β production in BMDCs (Schmitz et al., 2007). In the case of MV infection, IRF5 and IRF1 might be candidate transcription factors for MAVS-dependent and IRF3/IRF7-independent type I IFN induction in BMDCs.

In this context, we looked for possible transcription factors other than typical IRFs. We found from a pharmacological test that the treatment of CD150Tg/*Irf3*$^{-/-}$/*Irf7*$^{-/-}$ BMDCs with an NF-κB inhibitor (BAY11-7082) resulted a significant reduction of MV-induced *Ifn-β* mRNA expression (Supplemental Fig. 3), suggesting that NF-κB is involved in MV-induced type I IFN expression in BMDCs. The result infers that MV mouse models harbor multiple IFN-inducing pathways and the MAVS-NF-κB axis predominantly functions in transferred BMDCs even with no IRF3/IRF7 for protection against MV infection in mice. Yet, the possible participation of IRF1 or IRF5 in NF-κB-mediated type I IFN induction has remained to be determined. This MAVS-NF-κB-mediated IFN-β induction and resultant protection against MV spread is unique to mouse BMDCs: other immune cells are protected from MV by IFNAR-STAT signaling

in the MV-infected BMDC transfer system (Shingai et al., 2005). The result reflects the essential protective role of IFNAR (that is activated by primary MAVS-derived IFN-β) from establishing systemic MV infection in mouse models (Welstead et al., 2005; Shingai et al., 2005; Sellin et al., 2009; Koga et al., 2010).

Each successful virus species has developed its own means of circumventing the host IFN system, and the RNA-sensing system was developed in the course of stepwise mutation of the viral genomes. In an earlier study, RIG-I and MDA5 were reported to be sensors for RNA structures characteristic of virus species (Kato et al., 2006). This concept was adapted to MV in human epithelial cells (Ikegame et al., 2010). However, these typical cases appear rather rare in *in vivo* virus infections, which are more complicated than the situation found in RIG-I/MDA5 knockout mice (Kato et al., 2006), depending upon the host tropism, phases and stages of virus infection. *In vivo*, RIG-I and MDA5 in epithelial cells are implicated in the formation of an infectious milieu and type I IFN production in laboratory-adapted or genetically-mutated MV strains (Takaki et al., 2011; Shingai et al., 2005), but there appears to be no *in vivo* data supporting this finding. In general, each cell type has its own dominant IFN-inducing systems by which viral infections are differentially sensed and rapidly prevented in a cell-specific manner. Here, we show that the MAVS-dependent but IRF-3/7-independent IFN-β production actually does function in CD150Tg BMDCs in response to MV infection, this pathway being unique to BMDCs for primary MV protection. Secondary protection against MV spreading to other cells is accomplished by IFNAR which prevents systemic MV infection due to BMDCs transfer. There are a number of subsets in mouse DCs, which differentially respond to MV with their IFN-inducing pathways (Takaki et al., 2013). It will be of interest to determine whether the results are reproducible in other DC subsets in the mouse MV-infection model.

In patients with measles, alteration of the cytokine profile has been reported earlier (Griffin et al., 1990). The early Th1 response is shifted to a Th2 response, which occurs during the late stages of measles, with an increase in the secretion of IL-4 and a decrease in the IL-12 levels (Naniche and Oldstone, 2000; Atabani et al., 2001). Consistent with these reports, we detected a high level of IL-13 production in the coculture supernatant of $CD4^+$ T cells and MV-infected BMDCs (data not shown). The plasma level of the anti-inflammatory cytokine IL-10 is increased in patients with measles (Atabani et al., 2001; Yu et al., 2008). This elevated level of plasma IL-10 probably contributes to the impaired cellular immunity and depressed hypersensitivity response following MV infection (Ryon et al., 2002). However, the primary DC response and source of IL-10 in MV-infected patients is at present not clear.

Recently a study reported that IL-10 is the cause of MV-induced immunosuppression in MV-infectious model mice (Koga et al., 2010). However, during MV infection, both the cells which produce IL-10 and the induction mechanism of IL-10 in these cells have yet to be elucidated. In this report, we showed that $CD4^+$ T cells are one of the cell types that produce IL-10 in response to MV infection both *ex vivo* and *in vitro*. MV-infected BMDCs induce IL-10- and IFN-γ-producing $CD4^+$ T cells, but not Treg cells. Previous reports showed that T regulatory (Tr1) cells became IL-10 and IFN-γ producing $CD4^+$ T cells (Vieira et al., 2004; Roncarolo et al., 2006), and that Tr1 cells in concert with IL-10-producing DCs were indispensable for a high level of IL-10 (Roncarolo et al., 2006). However, in Fig. 4A, IL-10 was neither produced in BMDCs nor up-regulated in mouse sera irrespective of MV-infection. It is $CD4^+$ T cells that produce IL-10 in response to MV and CD3 stimulation (Fig. 4B).

Recent reports have demonstrated that IL-27 promotes IL-10 production by $CD4^+$ T cells (Stumhofer et al., 2007; Fitzgerald et al., 2007; Awasthi et al., 2007), and the induction of c-Maf, IL-21 and ICOS has been proposed as a mechanism of IL-27-mediated Tr1 cell differentiation (Pot et al., 2009). We examined whether IL-27 was involved in MV-induced IL-10 and IFN-γ production in $CD4^+$ T cells with an anti-IL-27p28 neutralizing antibody. Blocking IL-27p28 partially suppressed IL-10 production in $CD4^+$ T cells which had been cocultured with MV-infected BMDCs (Supplemental Fig. 6), indicating that IL-27 might participate in the mechanisms of induction of MV-mediated Tr1-like cells *in vitro*.

CD150Tg/*Mavs*$^{-/-}$ BMDCs completely lack the ability to produce type I IFN, and thereby are permissive to MV infection (Fig. 2A and B). CD150Tg/*Ifnar*$^{-/-}$ mice have the full capacity to produce IFN-β in MV infection, but cannot compensate for the IFNAR-null state in BMDCs. The artificial unresponsiveness of the IFN amplification pathway to MV infection may have caused unusual immune aberrations (Welstead et al., 2005; Shingai et al., 2005; Sellin et al., 2009; Koga et al., 2010) due to the absence of any "idling" production of type I IFN in these gene-disrupted mice (Takaoka and Taniguchi, 2003). It would be likely that a lack of the amplification pathway of type I IFN also confers MV permissiveness on BMDCs in mice, even though the mice have intact MAVS pathway to produce sufficient IFN-β. The present analysis of CD150Tg/*Mavs*$^{-/-}$ BMDCs in MV infection allowed us to highlight the molecular mechanisms of initial type I IFN induction and IL-10 production by $CD4^+$ T cells in a mouse model. Further analyses using the model will contribute to elucidation of possible mechanisms by which MV induces immune modulation.

Conflict of interest

There is no declared conflict of interest in this study.

Acknowledgements

We are grateful to Dr. Taniguchi (University of Tokyo) for providing *Irf3*$^{-/-}$ and *Irf7*$^{-/-}$ mice and Dr. Honda (RIKEN Research Center for Allergy and Immunology) for providing IL-10 Venus mice for this study. We also thank to Dr. Y. Yanagi (Kyushu University) for providing MV-luciferase. This work was supported in part by Grants-in-Aid from the Ministry of Education, Science, and Culture (Specified Project for Advanced Research) and the Ministry of Health, Labor, and Welfare of Japan, and by the Ono Foundation and the Itoh Foundation. Financial supports by the Program of Founding Research Centers for Emerging and Reemerging Infectious Diseases, MEXT, is gratefully acknowledged.

References

Akazawa, T., Ebihara, T., Okuno, M., Okuda, Y., Shingai, M., Tsujimura, K., Takahashi, T., Ikawa, M., Okabe, M., Inoue, N., Okamoto-Tanaka, M., Ishizaki, H., Miyoshi, J., Matsumoto, M., Seya, T., 2007. Antitumor NK activation induced by the Toll-like receptor 3-TICAM-1 (TRIF) pathway in myeloid dendritic cells. Proc. Natl. Acad. Sci. U. S. A. 104, 252–257, http://dx.doi.org/10.1073/pnas.0605978104.

Atabani, S.F., Byrnes, A.A., Jaye, A., Kidd, I.M., Magnusen, A.F., Whittle, H., Karp, C.L., 2001. Natural measles causes prolonged suppression of interleukin-12 production. J. Infect. Dis. 184, 1–9, http://dx.doi.org/10.1086/321009.

Atarashi, K., Tanoue, T., Shima, T., Imaoka, A., Kuwahara, T., Momose, Y., Cheng, G., Yamasaki, S., Saito, T., Ohba, Y., Taniguchi, T., Takeda, K., Hori, S., Ivanov, I.I., Umesaki, Y., Itoh, K., Honda, K., 2011. Induction of colonic regulatory T cells by indigenous Clostridium species. Science 331, 337–341, http://dx.doi.org/10.1126/science.1198469.

Awasthi, A., Carrier, Y., Peron, J.P., Bettelli, E., Kamanaka, M., Flavell, R.A., Kuchroo, V.K., Oukka, M., Weiner, H.L., 2007. A dominant function for interleukin 27 in generating interleukin 10-producing anti-inflammatory T cells. Nat. Immunol. 8, 1380–1389, http://dx.doi.org/10.1038/ni1541.

Daffis, S., Suthar, M.S., Szretter, K.J., Gale M.Jr., Diamond, M.S., 2009. Induction of IFN-beta and the innate antiviral response in myeloid cells occurs through an IPS-1-dependent signal that does not require IRF-3 and IRF-7. PLoS Pathog. 5, e1000607, http://dx.doi.org/10.1371/journal.ppat.1000607.

Ebihara, T., Shingai, M., Matsumoto, M., Wakita, T., Seya, T., 2008. Hepatitis C virus-infected hepatocytes extrinsically modulate dendritic cell maturation to activate T cells and natural killer cells. Hepatology 48 (July (1)), 48–58, http://dx.doi.org/10.1002/hep.22337.

Fitzgerald, D.C., Zhang, G.X., El-Behi, M., Fonseca-Kelly, Z., Li, H., Yu, S., Saris, C.J., Gran, B., Ciric, B., Rostami, A., 2007. Suppression of autoimmune inflammation of the central nervous system by interleukin 10 secreted by interleukin 27-stimulated T cells. Nat. Immunol. 8, 1372–1379, http://dx.doi.org/10.1038/ni1540.

Fugier-Vivier, I., Servet-Delprat, C., Rivailler, P., Rissoan, M.C., Liu, Y.J., Rabourdin-Combe, C., 1997. Measles virus suppresses cell-mediated immunity by interfering with the survival and functions of dendritic and T cells. J. Exp. Med. 186, 813–823, http://dx.doi.org/10.1084/jem.186.6.813.

Griffin, D.E., Ward, B.J., Jauregui, E., Johnson, R.T., Vaisberg, A., 1990. Immune activation during measles: interferon-gamma and neopterin in plasma and cerebrospinal fluid in complicated and uncomplicated disease. J. Infect. Dis. 161, 449–453.

Grosjean, I., Caux, C., Bella, C., Berger, I., Wild, F., Banchereau, J., Kaiserlian, D., 1997. Measles virus infects human dendritic cells and blocks their allostimulatory properties for CD4+ T cells. J. Exp. Med. 186, 801–812, http://dx.doi.org/10.1084/jem.186.6.801.

Honda, K., Takaoka, A., Taniguchi, T., 2006. Type I interferon gene induction by the interferon regulatory factor family of transcription factors. Immunity 25, 349–360.

Ikegame, S., Takeda, M., Ohno, S., Nakatsu, Y., Nakanishi, Y., Yanagi, Y., 2010. Both RIG-I and MDA5 RNA helicases contribute to the induction of alpha/beta interferon in measles virus-infected human cells. J. Virol. 84, 372–379, http://dx.doi.org/10.1128/JVI.01690-09.

Inaba, K., Inaba, M., Romani, N., Aya, H., Deguchi, M., Ikehara, S., Muramatsu, S., Steinman, R.M., 1992. Generation of large numbers of dendritic cells from mouse bone marrow cultures supplemented with granulocyte/macrophage colony-stimulating factor. J. Exp. Med. 176, 1693–1702.

Kato, H., Takeuchi, O., Sato, S., Yoneyama, M., Yamamoto, M., Matsui, K., Uematsu, S., Jung, A., Kawai, T., Ishii, K.J., Yamaguchi, O., Otsu, K., Tsujimura, T., Koh, C.S., Reis e Sousa, C., Matsuura, Y., Fujita, T., Akira, S., 2006. Differential roles of MDA5 and RIG-I helicases in the recognition of RNA viruses. Nature 441, 101–105, http://dx.doi.org/10.1038/nature04734.

Kawai, T., Akira, S., 2006. Innate immune recognition of viral infection. Nat. Immunol. 7, 131–137.

Kemper, C., Chan, A.C., Green, J.M., Brett, K.A., Murphy, K.M., Atkinson, J.P., 2003. Activation of human CD4+ cells with CD3 and CD46 induces a T-regulatory cell 1 phenotype. Nature 421, 388–392, http://dx.doi.org/10.1038/nature01315.

Koga, R., Ohno, S., Ikegame, S., Yanagi, Y., 2010. Measles virus-induced immunosuppression in SLAM knock-in mice. J. Virol. 84, 5360–5367, http://dx.doi.org/10.1128/JVI.02525-09.

Kobune, F., Sakata, H., Hayashi, T., 1990. Marmoset lymophoblastoid cells as a sensitive host for isolation of measles virus. J. Virol. 64, 700–705.

Lazear, H.M., Lancaster, A., Wilkins, C., Suthar, M.S., Huang, A., Vick, S.C., Clepper, L., Thackray, L., Brassil, M.M., Virgin, H.W., Nikolich-Zugich, J., Moses, A.V., Gale Jr., M., Früh, K., Diamond, M.S., 2013. IRF-3, IRF-5, and IRF-7 coordinately regulate the type I IFN response in myeloid dendritic cells downstream of MAVS signaling. PLoS Pathog. 9 (1), e1003118, http://dx.doi.org/10.1371/journal.ppat.1003118.

Marieí, I., Durbin, J.E., Levy, D.E., 1998. Differential viral induction of distinct interferon-a genes by positive feedback through interferon regulatory factor-7. EMBO J. 17, 6660–6669.

Matsumoto, M., Oshiumi, H., Seya, T., 2011. Antiviral responses induced by the TLR3 pathway. Rev. Med. Virol. 21, 67–77, http://dx.doi.org/10.1002/rmv.680.

Moss, W.J., Ota, M.O., Griffin, D.E., 2004. Measles: immune suppression and immune responses. Int. J. Biochem. Cell Biol. 36, 1380–1385, http://dx.doi.org/10.1016/j.biocel.2004.01.019.

Murabayashi, N., Kurita-Taniguchi, M., Ayata, M., Matsumoto, M., Ogura, H., Seya, T., 2002. Susceptibility of human dendritic cells (DCs) to measles virus (MV) depends on their activation stages in conjunction with the level of CDw150: role of Toll stimulators in DC maturation and MV amplification. Microbe. Infect. 4, 785–794.

Naniche, D., Oldstone, M.B., 2000. Generalized immunosuppression: how viruses undermine the immune response. Cell. Mol. Life Sci. 57, 1399–1407, http://dx.doi.org/10.1007/PL00000625.

Ohno, S., Ono, N., Takeda, M., Takeuchi, K., Yanagi, Y., 2004. Dissection of measles virus V protein in relation to its ability to block alpha/beta interferon signal transduction. J. Gen. Virol. 85, 2991–2999, http://dx.doi.org/10.1099/vir.0.80308-0.

Oshiumi, H., Matsumoto, M., Funami, K., Akazawa, T., Seya, T., 2003. TICAM-1, an adaptor molecule that participates in Toll-like receptor 3-mediated interferon-beta induction. Nat. Immunol. 4, 161–167, http://dx.doi.org/10.1038/ni886.

Oshiumi, H., Okamoto, M., Fujii, K., Kawanishi, T., Matsumoto, M., Koike, S., Seya, T., 2011. The TLR3/TICAM-1 pathway is mandatory for innate immune responses to poliovirus infection. J. Immunol. 187, 5320–5327, http://dx.doi.org/10.4049/jimmunol.1101503.

Panne, D., Maniatis, T., Harrison, S.C., 2007. An atomic model of the interferon-beta enhanceosome. Cell 129, 1111–1123, http://dx.doi.org/10.1016/j.cell.2007.05.019.

Pot, C., Jin, H., Awasthi, A., Liu, S.M., Lai, C.Y., Madan, R., Sharpe, A.H., Karp, C.L., Miaw, S.C., Ho, I.C., Kuchroo, V.K., 2009. IL-27 induces the transcription factor c-Maf, cytokine IL-21, and the costimulatory receptor ICOS that coordinately act together to promote differentiation of IL-10-producing Tr1 cells. J. Immunol. 183, 797–801, http://dx.doi.org/10.4049/jimmunol.0901233.

Radecke, F., Spielhofer, P., Schneider, H., Kaelin, K., Huber, M., Dötsch, C., Christiansen, G., Billeter, M.A., 1995. Rescue of measles viruses from cloned DNA. EMBO J. 14, 5773–5784.

Rathinam, V.A., Fitzgerald, K.A., 2011. Cytosolic surveillance and antiviral immunity. Curr. Opin. Virol. 1, 455–462, http://dx.doi.org/10.1016/j.coviro.2011.11.004.

Roncarolo, M.G., Gregori, S., Battaglia, M., Bacchetta, R., Fleischhauer, K., Levings, M.K., 2006. Interleukin-10-secreting type 1 regulatory T cells in rodents and humans. Immunol. Rev. 212, 28–50, http://dx.doi.org/10.1111/j.0105-2896.2006.00420.x.

Ryon, J.J., Moss, W.J., Monze, M., Griffin, D.E., 2002. Functional and phenotypic changes in circulating lymphocytes from hospitalized Zambian children with measles. Clin. Diagn. Lab. Immunol. 9, 994–1003, http://dx.doi.org/10.1128/CDLI.9.5.994-1003.2002.

Sato, M., Suemori, H., Hata, N., Asagiri, M., Ogasawara, K., Nakao, K., Nakaya, T., Katsuki, M., Noguchi, S., Tanaka, N., Taniguchi, T., 2000. Distinct and essential roles of transcription factors IRF-3 and IRF-7 in response to viruses for IFN-α/β gene induction. Immunity 13, 539–548, http://dx.doi.org/10.1016/S1074-7613(00)00053-4.

Schmitz, F., Heit, A., Guggemoos, S., Krug, A., Mages, J., Schiemann, M., Adler, H., Drexler, I., Haas, T., Lang, R., Wagner, H., 2007. Interferon-regulatory-factor 1 controls Toll-like receptor 9-mediated IFN-beta production in myeloid dendritic cells. Eur. J. Immunol. 37, 315–327.

Schneider-Schaulies, J., Dunster, L.M., Schneider-Schaulies, S., ter Meulen, V., 1995. Pathogenetic aspects of measles virus infections. Vet. Microbiol. 44, 113–125, http://dx.doi.org/10.1016/0378-1135(95)00004-T.

Schneider-Schaulies, S., Klagge, I.M., ter Meulen, V., 2003. Dendritic cells and measles virus infection. Curr. Top Microbiol. Immunol. 276, 77–101, http://dx.doi.org/10.1007/978-3-662-06508-2_4.

Sellin, C.I., Jégou, J.F., Renneson, J., Druelle, J., Wild, T.F., Marie, J.C., Horvat, B., 2009. Interplay between virus-specific effector response and Foxp3 regulatory T cells in measles virus immunopathogenesis. PLoS ONE 4, e4948, http://dx.doi.org/10.1371/journal.pone.0004948.

Servet-Delprat, C., Vidalain, P.O., Valentin, H., Rabourdin-Combe, C., 2003. Measles virus and dendritic cell functions: how specific response cohabits with immunosuppression. Curr. Top Microbiol. Immunol. 276, 103–123, http://dx.doi.org/10.1007/978-3-662-06508-2_5.

Shingai, M., Inoue, N., Okuno, T., Okabe, M., Akazawa, T., Miyamoto, Y., Ayata, M., Honda, K., Kurita-Taniguchi, M., Matsumoto, M., Ogura, H., Taniguchi, T., Seya, T., 2005. Wild-type measles virus infection in human CD46/CD150-transgenic mice: CD11c-positive dendritic cells establish systemic viral infection. J. Immunol. 175, 3253–3261.

Shingai, M., Ebihara, T., Begum, N.A., Kato, A., Honma, T., Matsumoto, K., Saito, H., Ogura, H., Matsumoto, M., Seya, T., 2007. Differential type I IFN-inducing abilities of wild-type versus vaccine strains of measles virus. J. Immunol. 179, 6123–6133.

Stumhofer, J.S., Silver, J.S., Laurence, A., Porrett, P.M., Harris, T.H., Turka, L.A., Ernst, M., Saris, C.J., O'Shea, J.J., Hunter, C.A., 2007. Interleukins 27 and 6 induce STAT3-mediated T cell production of interleukin 10. Nat. Immunol. 8, 1363–1371, http://dx.doi.org/10.1038/ni1537.

Takaki, H., Watanabe, Y., Shingai, M., Oshiumi, H., Matsumoto, M., Seya, T., 2011. Strain-to-strain difference of V protein of measles virus affects MDA5-mediated IFN-β-inducing potential. Mol. Immunol. 48, 497–504, http://dx.doi.org/10.1016/j.molimm.2010.10.006.

Takaki, H., Takeda, M., Tahara, M., Shingai, M., Oshiumi, H., Matsumoto, M., Seya, T., 2013. MyD88 pathway in plasmacytoid and CD4+ dendritic cells primarily triggers type I IFN production against measles virus in a mouse infection model. J. Immunol. (in press).

Takaoka, A., Taniguchi, T., 2003. New aspects of IFN-alpha/beta signalling in immunity, oncogenesis and bone metabolism. Cancer Sci. 94, 405–411, http://dx.doi.org/10.1111/j.1349-7006.2003.tb01455.x.

Takeda, M., Takeuchi, K., Miyajima, N., Kobune, F., Ami, Y., Nagata, N., Suzaki, Y., Nagai, Y., Tashiro, M., 2000. Recovery of pathogenic measles virus from cloned cDNA. J. Virol. 74, 6643–6647.

Takeda, M., Tahara, M., Hashiguchi, T., Sato, T.A., Jinnouchi, F., Ueki, S., Ohno, S., Yanagi, Y., 2007. A human lung carcinoma cell line supports efficient measles virus growth and syncytium formation via a SLAM- and CD46-independent mechanism. J. Virol. 81, 12091–12096, http://dx.doi.org/10.1128/JVI.01264-07.

Takeuchi, K., Kadota, S.I., Takeda, M., Miyajima, N., Nagata, K., 2003. Measles virus V protein blocks interferon (IFN)-alpha/beta but not IFN-gamma signaling by inhibiting STAT1 and STAT2 phosphorylation. FEBS Lett. 545, 177–182.

Tanabe, M., Kurita-Taniguchi, M., Takeuchi, K., Takeda, M., Ayata, M., Ogura, H., Matsumoto, M., Seya, T., 2003. Mechanism of up-regulation of human Toll-like receptor 3 secondary to infection of measles virus-attenuated strains. Biochem. Biophys. Res. Commun. 311, 39–48.

Tatsuo, H., Ono, N., Tanaka, K., Yanagi, Y., 2000. SLAM (CDw150) is a cellular receptor for measles virus. Nature 406, 893–897.

Thanos, D., Maniatis, T., 1995. Virus induction of human IFN beta gene expression requires the assembly of an enhanceosome. Cell 83, 1091–1100, http://dx.doi.org/10.1016/0092-8674(95)90136-1.

Vieira, P.L., Christensen, J.R., Minaee, S., O'Neill, E.J., Barrat, F.J., Boonstra, A., Barthlott, T., Stockinger, B., Wraith, D.C., O'Garra, A., 2004. IL-10-secreting regulatory T cells do not express Foxp3 but have comparable regulatory function to naturally occurring CD4+ CD25+ regulatory T cells. J. Immunol. 172, 5986–5993.

Welstead, G.G., Iorio, C., Draker, R., Bayani, J., Squire, J., Vongpunsawad, S., Cattaneo, R., Richardson, C.D., 2005. Measles virus replication in lymphatic cells and organs of CD150 (SLAM) transgenic mice. Proc. Natl. Acad. Sci. U. S. A. 102, 16415–16420, http://dx.doi.org/10.1073/pnas.0505945102.

Yoneyama, M., Onomoto, K., Fujita, T., 2008. Cytoplasmic recognition of RNA. Adv. Drug. Deliv. Rev. 60, 841–846, http://dx.doi.org/10.1016/j.addr.2007.12.001.

Yu, X.L., Cheng, Y.M., Shi, B.S., Qian, F.X., Wang, F.B., Liu, X.N., Yang, H.Y., Xu, Q.N., Qi, T.K., Zha, L.J., Yuan, Z.H., Ghildyal, R., 2008. Measles virus infection in adults induces production of IL-10 and is associated with increased CD4+ CD25+ regulatory T cells. J. Immunol. 181, 7356–7366.

The MyD88 Pathway in Plasmacytoid and CD4$^+$ Dendritic Cells Primarily Triggers Type I IFN Production against Measles Virus in a Mouse Infection Model

Hiromi Takaki,* Makoto Takeda,† Maino Tahara,† Masashi Shingai,*,[1] Hiroyuki Oshiumi,* Misako Matsumoto,* and Tsukasa Seya*

Infection by measles virus (MV) induces type I IFN via the retinoic acid–inducible gene I/melanoma differentiation–associated gene 5/mitochondrial antiviral signaling protein (MAVS) pathway in human cells. However, the in vivo role of the MAVS pathway in host defense against MV infection remains undetermined. CD150 transgenic (Tg) mice, which express human CD150, an entry receptor for MV, with the disrupting IFNR gene (*Ifnar*$^{-/-}$), are susceptible to MV and serve as a model for MV infection. In this study, we generated CD150Tg/*Mavs*$^{-/-}$ mice and examined MV permissiveness compared with that in CD150Tg/*Ifnar*$^{-/-}$ mice. MV replicated mostly in the spleen of i.p.-infected CD150Tg/*Ifnar*$^{-/-}$ mice. Strikingly, CD150Tg/*Mavs*$^{-/-}$ mice were not permissive to MV in vivo because of substantial type I IFN induction. MV barely replicated in any other organs tested. When T cells, B cells, and dendritic cells (DCs) isolated from CD150Tg/*Mavs*$^{-/-}$ splenocytes were cultured with MV in vitro, only the DCs produced type I IFN. In vitro infection analysis using CD150Tg/*Mavs*$^{-/-}$ DC subsets revealed that CD4$^+$ and plasmacytoid DCs, but not CD8α$^+$ and CD8α$^-$CD4$^-$ double negative DCs, were exclusively involved in type I IFN production in response to MV infection. Because CD150Tg/*Mavs*$^{-/-}$ mice turned permissive to MV by anti-IFNAR Ab, type I IFN produced by CD4$^+$ DCs and plasmacytoid DCs plays a critical role in antiviral protection for neighboring cells expressing IFNAR. Induction of type I IFN in these DC subsets was abolished by the MyD88 inhibitory peptide. Thus, production of type I IFN occurs via the MyD88-dependent and MAVS-independent signaling pathway during MV infection. *The Journal of Immunology*, **2013, 191: 4740–4747.**

Type I IFNs (IFN-α/β) are crucial for protection against viral infections (1). Viral RNA is detected by cytosolic RNA sensors and induces expression of type I IFN (2). Extracellular dsRNA of a virus product is detected by the endosomal TLR3, whereas intracellular dsRNA is sensed by the retinoic acid–inducible gene I (RIG-I) and the melanoma differentiation–associated gene 5 (MDA5) (3). Upon recognizing dsRNA, TLR3 recruits the Toll/IL-1R (TIR) homology domain–containing adaptor molecule 1 (TICAM-1, also referred to as TRIF) and induces type I IFN production (4, 5). The RIG-I–like receptors (RLRs), RIG-I and MDA5, signal via the mitochondrial antiviral signaling protein (MAVS; also known as VISA, Cardif, or IPS-1) and also induce type I IFN expression (6). Knocking out these adaptor molecules results in failure to activate the transcription factors IFN regulatory factor (IRF)-3 and IRF-7, leading to an incompetence in type I IFN production and antiviral host defense (3, 7, 8). Type I IFN induction following the recognition of measles virus (MV) RNA is dependent on the RIG-I/MDA5-MAVS pathway in human epithelial cell lines (9, 10). However, the role of the RIG-I/MDA5-MAVS pathway during in vivo MV infection remains undetermined.

MV, of the genus *Morbillivirus* from the Paramyxoviridae family, is a highly pathogenic, nonsegmented negative single-stranded RNA virus that causes respiratory distress and immunosuppression in humans (11). Wild-type strains of MV enter cells via human CD150, which is also referred to as signaling lymphocyte activation molecule (12), and human poliovirus receptor–like protein 4 (13, 14). Expression of these receptors is restricted either to activated lymphocytes, dendritic cells (DCs), and macrophages for CD150 or to the basolateral surface of epithelial cells for PVRL4 (15). Among these cell populations, CD11c$^+$ DCs and alveolar macrophages (AMs) are reported to be the first target cells of early-phase MV infection in the CD150 transgenic (Tg) mouse model (16, 17) and in nonhuman primates (18, 19). Moreover, DCs are found to be involved in pathogenesis and immunosuppression during and after acute MV infection (20, 21). However, it is unclear how DCs and macrophages recognize MV RNA to produce type I IFN.

Human CD150Tg mice, which are slightly permissive to MV, are used to study host responses against MV infection in vivo (16, 22–24). CD150Tg/*Ifnar*$^{-/-}$ mice, which are generated by crossing CD150Tg mice with *Ifnar*$^{-/-}$ mice, are susceptible to MV infection

*Department of Microbiology and Immunology, Graduate School of Medicine, Hokkaido University, Kita-ku, Sapporo 060-8638, Japan; and †Department of Virology 3, National Institute of Infectious Diseases, Gakuen 4-7-1, Musashimurayama, Tokyo 208-0011, Japan

[1]Current address: Laboratory of Molecular Microbiology, National Institute of Allergy and Infectious Diseases, National Institutes of Health, Bethesda, MD.

Received for publication July 3, 2013. Accepted for publication August 28, 2013.

This work was supported in part by grants-in-aid from the Ministry of Education, Science, and Culture (Specified Project for Advanced Research) and the Ministry of Health, Labor, and Welfare of Japan; the Japan Society for the Promotion of Science Fellows and Support Office for Female Researchers in Hokkaido University; the Takeda Foundation and the Waxmann Foundation; and the Program of Founding Research Centers for Emerging and Reemerging Infectious Diseases, Ministry of Education, Culture, Sports, Science and Technology.

Address correspondence and reprint requests to Prof. Tsukasa Seya and Dr. Hiromi Takaki, Department of Microbiology and Immunology, Hokkaido University Graduate School of Medicine, Kita 15, Nishi 7, Kita-ku, Sapporo 060-8638, Japan. E-mail addresses: seya-tu@pop.med.hokudai.ac.jp (T.S.) and tahiromi@sci.hokudai.ac.jp (H.T.)

The online version of this article contains supplemental material.

Abbreviations used in this article: AM, alveolar macrophage; BMDC, bone marrow–derived DC; cDC, conventional DC; DC, dendritic cell; DN, double negative; IRF, IFN regulatory factor; LN, lymph node; MAVS, mitochondrial antiviral signaling protein; MDA5, melanoma differentiation–associated gene 5; MOI, multiplicity of infection; MV, measles virus; MyD88, myeloid differentiation factor 88; pDC, plasmacytoid DC; PDCA-1, pDC Ag 1; RIG-I, retinoic acid–inducible gene I; RLR, RIG-I–like receptor; Tg, transgenic; TICAM-1, Toll/IL-1R homology domain–containing adaptor molecule 1; TIR, Toll/IL-1R.

and serve as a useful mouse model (16, 24). In the current study, using the CD150Tg mouse model in combination with *Mavs*$^{-/-}$, *Irf3*$^{-/-}$/*Irf7*$^{-/-}$, and *Ticam1*$^{-/-}$ mice, we found that CD150Tg/*Mavs*$^{-/-}$ mice were not permissive to MV in vivo, whereas CD150Tg/*Irf3*$^{-/-}$/*Irf7*$^{-/-}$ mice were permissive. Furthermore, CD150Tg/*Mavs*$^{-/-}$ plasmacytoid DCs (pDCs) and CD4$^+$ DCs produced type I IFN in response to MV infection in vitro. Analysis using the myeloid differentiation factor 88 (MyD88) inhibitory peptide and MyD88$^{-/-}$ mice revealed that type I IFN production in these DC subsets was dependent on the MyD88 pathway. To our knowledge, this is the first study to show that type I IFN induction in MV-infected mouse DCs depends on the MyD88 pathway. The properties of the MV-permissive mouse DC subsets may be crucial for ensuring immune response, including immunosuppression during MV infection.

Materials and Methods

Mice

All mice were backcrossed to C57BL/6 mice more than eight times before use. CD150Tg (16), *Ticam1*$^{-/-}$ (25), and *Mavs*$^{-/-}$ (26) mice were generated in our laboratory. *Irf3*$^{-/-}$ and *Irf7*$^{-/-}$ mice were provided by Dr. T. Taniguchi (University of Tokyo, Tokyo, Japan). *Myd88*$^{-/-}$ mice were provided by Drs. K. Takeda and S. Akira (Osaka University, Osaka, Japan). All mice were maintained under specific pathogen–free conditions in the Animal Facility at Hokkaido University Graduate School of Medicine (Sapporo, Japan) and used when they were between 6 and 12 wk of age. This study was carried out in strict accordance with the recommendations in the National Institutes of Health *Guide for the Care and Use of Laboratory Animals*. The protocol was approved by the Committee on the Ethics of Animal Experiments in the Animal Safety Center, Hokkaido University. All mice were used according to the guidelines of the Institutional Animal Care and Use Committee of Hokkaido University, which approved this study as no.13-0024. All inoculation and experimental manipulation were performed with the animals under anesthesia that was induced and maintained with pentobarbital sodium, and all efforts were made to minimize suffering.

Virus and cell culture

Vero/CD150 cells were maintained in DMEM supplemented with 10% heat-inactivated FBS and antibiotics. IC323, corresponding to the IC-B strain of MV (27), was recovered from the plasmid p(+)MV323 encoding the antigenomic IC-B sequence (28). IC323-Luci (MV-luciferase), which expresses the reporter *Renilla* luciferase from the first gene position of the MV genome, was a kind gift from Dr. Y. Yanagi (Kyushu University, Fukuoka, Japan) (29). MV-luciferase was maintained in Vero/CD150 cells (30). Virus titer was determined as PFUs on Vero/CD150, and the multiplicity of infection (MOI) of each experiment was calculated based on this titer (27). Splenic CD19$^+$, CD4$^+$, CD8$^+$ cells, and CD11c$^+$ DCs were isolated using anti-CD19, anti-CD4, anti-CD8, and anti-CD11c MACS beads (Miltenyi Biotec). Splenic CD8α$^+$ DCs, CD4$^+$ DCs, and double negative (DN) DCs were isolated using CD8α$^+$ or CD4$^+$ DC isolation kits (Miltenyi Biotec) according to the manufacturer's instructions. For isolation of pDCs and conventional DCs (cDCs), spleens were treated with 400 IU Mandle U/ml collagenase D (Roche) at 37°C for 25 min in HBSS (Sigma-Aldrich). EDTA was added, and the cell suspension was incubated for an additional 5 min at 37°C. After removal of RBCs with ammonium chloride–potassium lysis buffer, CD11c$^+$ DCs were isolated using CD11c MACS beads. MACS-sorted DCs were stained with anti-CD11b–FITC, anti-pDC Ag 1 (PDCA-1)–PE (eBioscience), and anti-CD11c–allophycocyanin (BioLegend) and sorted using a FACSAria II (BD). The purity of sorted cells was > 98%.

FACS analysis

For pDC staining, splenocytes were stained with anti-CD11c–allophycocyanin (BioLegend), anti–PDCA-1–PE (BioLegend), and anti-human CD150–FITC (eBiosciences). For CD4$^+$ DCs, CD8$^+$ DCs, and DN DCs staining, splenocytes were stained with anti-CD11c–allophycocyanin (BioLegend), anti-CD4–PerCP (BioLegend), anti-CD8–PE (BioLegend), and anti-human CD150–FITC. For B cell staining, splenocytes were stained with anti-B220–allophycocyanin (BioLegend), anti-CD19–PE (BioLegend), and anti-human CD150–FITC. For T cell staining, anti-CD3–allophycocyanin (BioLegend), anti-CD4–PerCP, anti-CD8–PE, and anti-human CD150–FITC were used. Fluorescence intensity of CD150 was measured by flow cytometry. For TLR7 intracellular staining in pDCs, DCs were stained with anti-TLR7–FITC (IMGENEX), anti-CD11c–allophycocyanin, and anti–PDCA-1–PE using the BD Cytofix/Cytoperm Kit (BD Biosciences). For TLR7 intracellular staining in CD4$^+$, CD8$^+$, and DN DCs, DCs were stained with anti-TLR7–FITC (IMGENEX), anti-CD11c–allophycocyanin, anti-CD4–PerCP, and anti-CD8–PE, using the BD Cytofix/Cytoperm Kit (BD Biosciences). Stained cells were analyzed by flow cytometry.

Experimental infection and luciferase assay

Mice were infected i.p. with MV-luciferase at the indicated doses. For in vivo blockade of the type I IFNR, mice were i.p. injected with 2.5 mg MAR1-5A3, a mAb against IFNAR-1 (BioLegend), 1 d prior to infection. Tissues were collected from the mice at different time points, and the efficiency of infection was measured by luciferase assay. Cells (1×10^7) from various tissues were harvested in 100 μl lysis buffer. The amount of protein in each lysate was determined by bicinchoninic acid assay. Luciferase assay was performed using a Dual-Luciferase Reporter Assay System (Promega), and luciferase activity was read using a Lumat LB 9507 (Berthold Technologies). To measure the efficiency of in vitro infection, cells (5×10^4–4×10^5) were harvested in 25 μl lysis buffer for luciferase assay. For MyD88 inhibition assay, cells were pretreated with 50 μM MyD88 inhibitory peptide (RQIKIWFQNRRMKWKK-RDVLPGTCVNS-NH2; InvivoGen) or the control peptide (RQIKIWFQNRRMKWKK-SLHGRGDPMEAFII-NH2; InvivoGen) for 6 h, and then cells were infected with MV. MyD88 inhibitory peptide contains a sequence from the MyD88 TIR homodimerization domain (RDVLPGT) preceded with a protein transduction sequence (RQIKIWFQNRRMKWKK) derived from antennapedia, which enables the peptide to translocate through the cell membrane. For intratracheal infection with MV, mice were anesthetized and injected with MV-luciferase (8×10^5 PFU/50 μl in PBS) intratracheally. At 3 d after inoculation, mice were sacrificed and perfused with PBS containing 10 mM EDTA from the right ventricle. Lung lobes were isolated, and collagenase buffer [150 U/ml collagenase D (Roche), 10 μg/ml DNase I (Takara), and 5% FCS in RPMI 1640 medium] was injected into the lobes, using a 27-gauge needle. The lobes were then shredded into small pieces and incubated at 37°C for 45 min. During the last 5 min, EDTA was added at 10 mM. Any remaining small pieces were dispersed by passage in and out through a 20-gauge needle, and the suspension was passed through nylon mesh to remove debris. A single-cell suspension was prepared after RBC lysis. A total of 2×10^6 cells were harvested in 100 μl lysis buffer for luciferase assay.

ELISA

Culture supernatants of cells ($1–5 \times 10^5$) seeded on 96-well plates were collected and analyzed for cytokine levels, using ELISA. ELISA kits for mouse IFN-α and IFN-β were from PBL Biomedical Laboratories. Assays were performed according to the manufacturer's instructions.

RT-PCR and real-time PCR

Total RNA was prepared using TRIzol Reagent (Invitrogen) following the manufacturer's instructions. RT-PCR was carried out using a High Capacity cDNA Reverse Transcription Kit (Applied Biosystems) according to the manufacturer's instructions. Real-time PCR was performed using a StepOne Real-Time PCR System (Applied Biosystems). The following oligonucleotides were used for *β-actin*: 5′-TTTGCAGCTCCTTCGTTGC-3′ and 5′-TCGTCATCCATGGCGAACT-3′; for *Ifn-β*: 5′-CCAGCTCCAAGAAAGGACGA-3′ and 5′-CGCCCTGTAGGTGAGGTTGAT-3′; for *Ifn-α4*: 5′-CTGCTGGCTGTGAGGACATACT-3′ and 5′-AGGCACAGAGGCTGTGTTTCTT-3′; for *Ifit1*: 5′-TGTGCTGAGATGGACTGTGAG-3′ and 5′-TTTCTGGCTCCACTTTCAGAG-3′; for *Cxcl10*: 5′-GTGTTGAGATCATTGCCACGA-3′ and 5′-GCGTGGCTTCACTCCAGTTAA-3′; for *Tlr7*: 5′-GTATGCCGCCAAATCTAAAG-3′ and 5′-GGCTGAGGTCCAAAATTTCC-3′; and for *MV-P*: 5′-cTGCATCACGCAGTGTAATC-3′ and 5′-CTGGTGGAACTTGGCAAGATC-3′. Levels of target mRNAs were normalized to *β-actin*, and fold-induction of transcripts was calculated using the ddCT method relative to unstimulated cells.

Statistical analyses

Statistical significance of differences between groups was determined by the Student *t* test using Microsoft Excel software. The *p* values < 0.05 were considered significant.

Results

CD150Tg/Mavs$^{-/-}$ *mice are not permissive to MV*

To quantitate the efficiency of MV infection, we used a recombinant MV-luciferase that expresses the reporter *Renilla* luciferase from the insert of the MV genome (29). CD150 expression levels did

not differ among various spleen cells from CD150Tg, CD150Tg/*Ifnar*$^{-/-}$, CD150Tg/*Irf3*$^{-/-}$/*Irf7*$^{-/-}$, CD150Tg/*Ticam1*$^{-/-}$ or CD150Tg/*Mavs*$^{-/-}$ mice (Supplemental Fig. 1). Each knockout mouse strain was i.p. injected with 1×10^6 PFU of MV-luciferase. In accord with previous data (16, 22), luciferase activity in various tissues derived from MV-infected CD150Tg mice was very low 2 d after inoculation (Fig. 1A). In contrast, luciferase activity was predominantly increased in spleen and lymph nodes (LNs) derived from MV-infected CD150Tg/*Ifnar*$^{-/-}$ mice, compared with other tissues (Fig. 1A). *MV-P* mRNA expression was also increased in MV-infected CD150Tg/*Ifnar*$^{-/-}$ spleen and LNs, similarly to luciferase activity (Fig. 1B). These results indicate that spleen and LNs are the major target tissues of i.p.-injected MV in CD150Tg/*Ifnar*$^{-/-}$ mice, as shown in a previous report (24). Luciferase activity was increased in the lung of CD150Tg/*Ifnar*$^{-/-}$, but not CD150Tg/*Mavs*$^{-/-}$, mice after intratracheal injection of MV

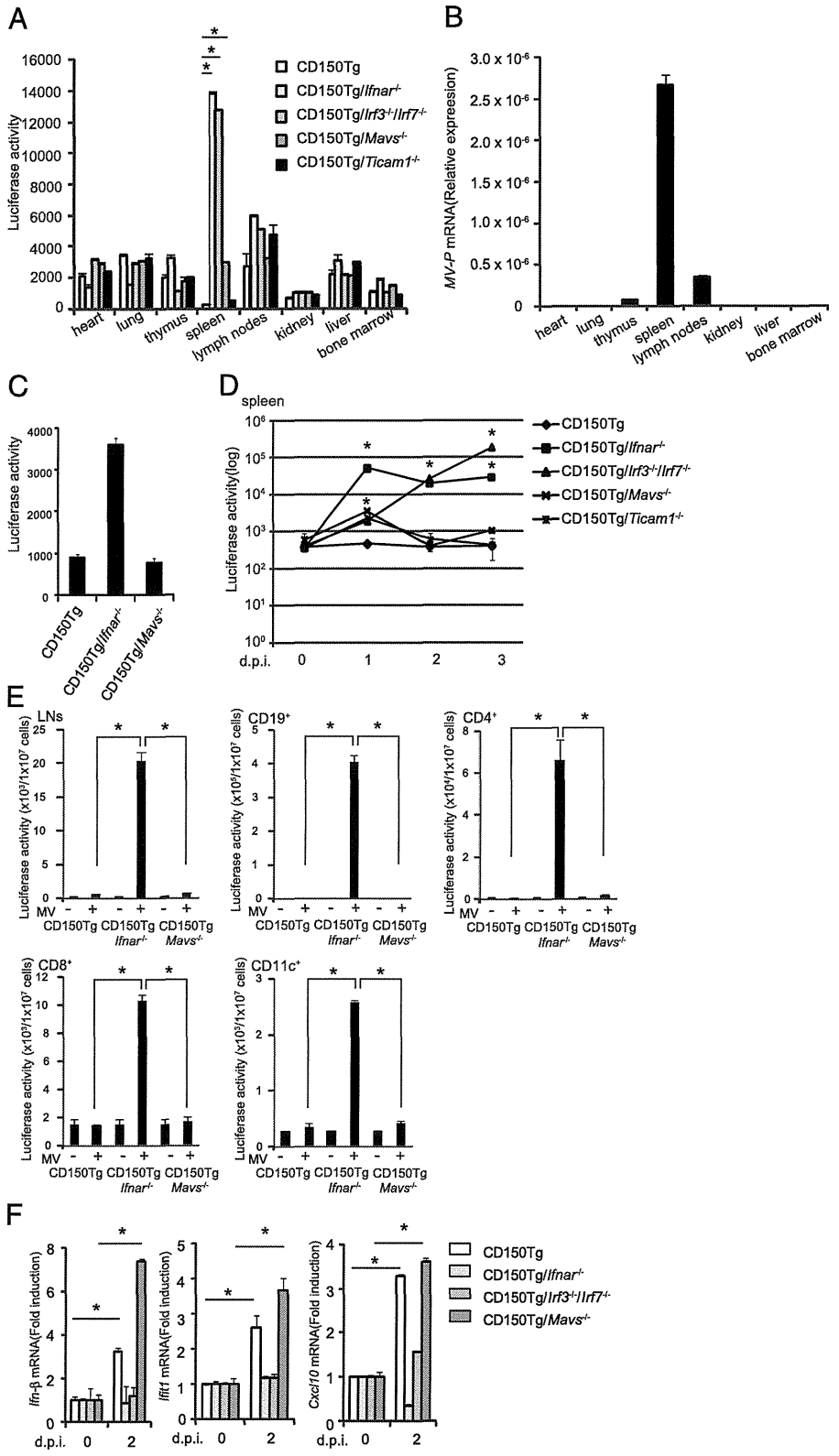

FIGURE 1. CD150Tg/*Mavs*$^{-/-}$ mice were resistant to in vivo MV infection. (**A**) CD150Tg, CD150Tg/*Ifnar*$^{-/-}$, CD150Tg/*Irf3*$^{-/-}$/*Irf7*$^{-/-}$, CD150Tg/*Mavs*$^{-/-}$, and CD150Tg/*Ticam1*$^{-/-}$ mice were infected i.p. with 1×10^6 PFU MV-luciferase. After 2 d, cells were isolated from each organ and lysed with lysis buffer for luciferase assay. The amount of protein in each lysate was determined by bicinchoninic acid assay. Luciferase activity in each lysate was measured and normalized by the amount of protein. Data are shown as luciferase activity per 1 mg of protein and means ± SD of three independent samples. *$p < 0.05$. (**B**) CD150Tg/*Ifnar*$^{-/-}$ mice were infected with MV (1×10^6 PFU). At 2 d after inoculation, total RNA was collected from the indicated tissues, and the expression level of *MV-P* mRNA in each tissue was determined by real-time PCR. *MV-P* mRNA expression is shown as expression relative to *β-actin*. Data are means ± SD of three independent samples. (**C**) CD150Tg, CD150Tg/*Ifnar*$^{-/-}$, and CD150Tg/*Mavs*$^{-/-}$ mice were intratracheally injected with MV-luciferase (8×10^5 PFU). At 3 d after inoculation, luciferase activity was measured in cells from lungs. Data are means ± SD of two independent samples. (**D**) At the indicated days post infection (d.p.i.), luciferase activity in 1×10^7 splenocytes was measured. Three mice were analyzed for each genotype. Data are representative of two independent experiments. *$p < 0.05$ versus CD150Tg. (**E**) CD150Tg, CD150Tg/*Ifnar*$^{-/-}$, and CD150Tg/*Mavs*$^{-/-}$ mice were infected i.p. with 1×10^6 PFU MV-luciferase. At 2 d.p.i., CD19$^+$, CD4$^+$, CD8$^+$, and CD11c$^+$ cells were isolated from splenocytes, using anti-CD19, anti-CD4, anti-CD8, and anti-CD11c MACS beads. Luciferase activity in CD19$^+$, CD4$^+$, CD8$^+$, and CD11c$^+$ cells, as well as LNs, was measured and normalized by the total number of cells. Data are shown as the luciferase activity per 1×10^7 cells. Data are means ± SD of three independent samples. *$p < 0.05$. (**F**) CD150Tg, CD150Tg/*Ifnar*$^{-/-}$, CD150Tg/*Irf3*$^{-/-}$/*Irf7*$^{-/-}$, and CD150Tg/*Mavs*$^{-/-}$ mice were infected i.p. with 1×10^6 PFU MV-luciferase. At 2 d.p.i., mRNA levels of *Ifn-β*, *Ifit1*, and *Cxcl10* in spleens were determined by real time-PCR. Data are means ± SD of three independent samples. *$p < 0.05$.

(Fig. 1C). However, the route of MV administration is an issue to be further investigated.

In MV-infected human epithelial cells, signals via RIG-I and MDA5 are essential for production of type I IFN (9, 10). Cells lacking the MAVS protein, a common adaptor molecule for RIG-I and MDA5, are unable to produce type I IFN in response to members of the Paramyxoviridae family (8). To investigate the in vivo role of the MAVS pathway during MV infection, we first examined whether CD150Tg/*Mavs*$^{-/-}$ mice were permissive to MV infection. Although luciferase activity in splenocytes was slightly increased in CD150Tg/*Mavs*$^{-/-}$ mice compared with CD150Tg mice 1 d after i.p. inoculation, luciferase activity in splenocytes of CD150Tg/*Mavs*$^{-/-}$ mice was decreased to the same degree as in those of CD150Tg mice a few days after inoculation (Fig. 1A, 1D, 1E). In contrast, luciferase activity in splenocytes was significantly increased in CD150Tg/*Ifnar*$^{-/-}$ and CD150Tg/*Irf3*$^{-/-}$/*Irf7*$^{-/-}$ mice compared with CD150Tg, CD150Tg/*Mavs*$^{-/-}$, or CD150Tg/*Ticam1*$^{-/-}$ mice 2 d after inoculation (Fig. 1D). We also examined luciferase activity in LNs and CD4$^+$, CD8$^+$, CD19$^+$, and CD11c$^+$ cells isolated from splenocytes of the mice. As shown in Fig. 1E, luciferase activity in these cells from MV-infected CD150Tg/*Mavs*$^{-/-}$ mice was much lower than in those from CD150Tg/*Ifnar*$^{-/-}$ mice. To investigate the reasons why CD150Tg/*Mavs*$^{-/-}$ mice were resistant to MV infection, we examined the expression level of mRNA coding antiviral protein in splenocytes (Fig. 1F). The expression of *Ifn-β* and two IFN-inducible genes, *Ifit1* and *Cxcl10*, was upregulated by MV infection in splenocytes from CD150Tg/*Mavs*$^{-/-}$ mice, but not in those from CD150Tg/*Ifnar*$^{-/-}$ and CD150Tg/*Irf3*$^{-/-}$/*Irf7*$^{-/-}$ mice (Fig. 1F). Type I IFN levels in sera were below the detection limit throughout the time course (data not shown). These data suggest that in vivo MV infection induces the expression of type I IFN and IFN-inducible genes to elicit resistance to MV infection in CD150Tg/*Mavs*$^{-/-}$. Moreover, type I IFN induction by in vivo MV infection occurs via the IRF3/IRF7-dependent and MAVS-independent pathway.

Next, we performed in vivo infection experiments using IFNAR Ab. Type I IFNR in CD150Tg/*Mavs*$^{-/-}$ mice was blocked by injecting 2.5 mg of the MAR1-5A3 mAb against IFNAR-1, 1 d before infection. This dose of Ab is reported to block antiviral effects of type I IFN in vivo (31). In MV-infected CD150Tg/*Mavs*$^{-/-}$ mice, blocking of IFNAR increased luciferase activity in LNs up to 180-fold, and in splenocytes up to 10-fold (Fig. 2A). Similarly, luciferase activity was increased up to 6-fold in CD19$^+$, 8-fold in CD4$^+$, 29-fold in CD8$^+$, and 17-fold in CD11c$^+$ cells by IFNAR blocking (Fig. 2B). These results indicate that CD150Tg/*Mavs*$^{-/-}$ mice are permissive to MV infection once IFNAR is functionally neutralized.

CD11c$^+$ DCs produce type I IFN via the MAVS-independent pathway during MV infection

To determine which cell types were responsible for type I IFN induction in MV-infected CD150Tg/*Mavs*$^{-/-}$ mice, we performed an in vitro infection assay using splenocytes. When infected with MV in vitro, the luciferase activity in B cells and T cells isolated from CD150Tg/*Mavs*$^{-/-}$ mice was comparable to activity in those from CD150Tg/*Ifnar*$^{-/-}$ mice (Fig. 3A). Treatment with anti-IFNAR Ab did not affect the infection efficiency in CD150Tg/*Mavs*$^{-/-}$ T and B cells (Fig. 3A). Unlike T and B cells, CD150Tg/*Mavs*$^{-/-}$ CD11c$^+$ DCs were not permissive to MV (Fig. 3A). These data suggest that CD11c$^+$ DCs, but not lymphocytes, are responsible for resistance to MV infection in CD150Tg/*Mavs*$^{-/-}$ mice. Because CD150Tg/*Mavs*$^{-/-}$ mice were permissive to MV in vivo when type I IFN signaling was blocked by anti-IFNAR Ab

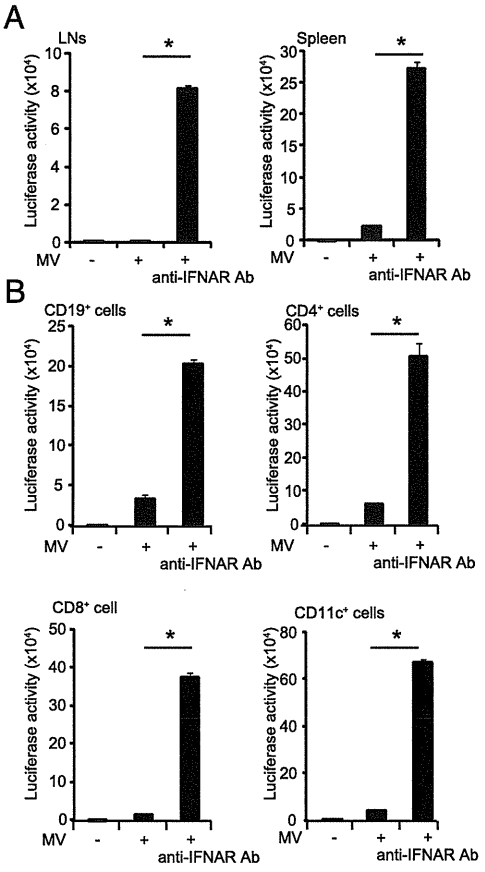

FIGURE 2. CD150Tg/*Mavs*$^{-/-}$ mice were permissive to MV after treatment with anti-IFNAR Ab in vivo. CD150Tg/*Mavs*$^{-/-}$ mice were injected i.p. with 2.5 mg of anti-IFNAR Ab at 1 d before MV-luciferase infection (1×10^7 PFU per mouse). At 2 d post infection, luciferase activity in LNs, splenocytes (**A**), and (**B**) CD19$^+$, CD4$^+$, CD8$^+$, and CD11c$^+$ cells isolated from splenocytes was measured and normalized by the total number of cells. Data are shown as the luciferase activity per 1×10^7 cells. Data are means ± SD of three independent samples. *$p < 0.05$.

(Fig. 2A, 2B), we examined whether treatment with anti-IFNAR Ab increased the efficiency of MV infection in vitro. CD150Tg/*Mavs*$^{-/-}$ CD11c$^+$ DCs were permissive to MV in the presence of anti-IFNAR Ab (Fig. 3A). Consistent with results in Fig. 3A, type I IFN was detectable in the culture supernatant of MV-infected CD150Tg/*Mavs*$^{-/-}$ CD11c$^+$ DCs, but not of T or B cells (Fig. 3B and data not shown). Expression of *Ifn-β* and *Ifn-α4* mRNAs in CD150Tg/*Mavs*$^{-/-}$ CD11c$^+$ DCs was also upregulated within 6 h after MV infection (Fig. 3C). These data suggest that CD11c$^+$ DCs, but neither T nor B cells, mainly produce type I IFN through the MAVS-independent pathway in response to MV infection in vitro.

CD4$^+$ DCs and pDCs are responsible for MV-induced type I IFN production in CD150Tg/Mavs$^{-/-}$ *mice*

Our data indicate that type I IFN induction following the MV recognition in mouse DCs is independent of the MAVS pathway. Various types of DCs have been identified in mouse secondary lymphoid tissues, including three CD11c^{high} subsets: CD8α$^+$, CD4$^+$, and DN CD4$^-$CD8α$^-$ DCs (32), and one subset of CD11c^{low} pDCs (33). To identify the type I IFN-producing subsets, we used a cell sorter to isolate CD11c^{high} (cDCs) and CD11c^{low} pDCs from splenocytes, with purity > 98% (data not shown). CD150Tg/*Ifnar*$^{-/-}$ cDCs and pDCs were permissive to MV (Fig. 4A and 4C). In contrast, both CD150Tg/*Mavs*$^{-/-}$ cDCs and pDCs